ANTIOXIDANTS & REDOX SIGNALING
Volume 19, Number 1, 2013

DOI: 10.1089/ars.2012.5024

Discoveries

REBOUND ORIGINAL RESEARCH COMMUNICATION

Hydrogen Sulfide Treatment Promotes Glucose Uptake by Increasing Insulin Receptor Sensitivity and Ameliorates Kidney Lesions in Type 2 Diabetes

Rong Xue,[1,*] Dan-Dan Hao,[1,*] Ji-Ping Sun,[1,*] Wen-Wen Li,[1] Man-Man Zhao,[1] Xing-Hui Li,[1] Ying Chen,[1] Jian-Hua Zhu,[2] Ying-Jiong Ding,[1] Jun Liu,[1] and Yi-Chun Zhu[1]

Abstract

Aims: To examine if hydrogen sulfide (H_2S) can promote glucose uptake and provide amelioration in type 2 diabetes. ***Results:*** Treatment with sodium hydrosulfide (NaHS, an H_2S donor) increased glucose uptake in both myotubes and adipocytes. The H_2S gas solution showed similar effects. The NaHS effects were blocked by an siRNA-mediated knockdown of the insulin receptor (IR). NaHS also increased phosphorylation of the IR, PI3K, and Akt. In Goto-Kakizaki (GK) diabetic rats, chronic NaHS treatment ($30\ \mu mol \cdot kg^{-1} \cdot day^{-1}$) decreased fasting blood glucose, increased insulin sensitivity, and increased glucose tolerance with increased phosphorylation of PI3K and Akt in muscles. Similar insulin-sensitizing effects of NaHS treatment were also observed in Wistar rats. Moreover, glucose uptake was reduced in the cells with siRNA-mediated knockdown of the H_2S-generating enzyme cystathionine γ-lyase in the presence or absence of exogenous H_2S. Moreover, chronic NaHS treatment reduced oxygen species and the number of crescentic glomeruli in the kidney of GK rats. ***Innovation and Conclusion:*** This study provides the first piece of evidence for the insulin-sensitizing effect of NaHS/H_2S in the both *in vitro* and *in vivo* models of insulin resistance. ***Rebound Track:*** This work was rejected during a standard peer review and rescued by the Rebound Peer Review (*Antoxid Redox Signal* 16: 293–296, 2012) with the following serving as open reviewers: Jin-Song Bian, Samuel Dudley, Hideo Kimura, and Xian Wang. *Antioxid. Redox Signal*. 19, 5–23.

Introduction

Hydrogen sulfide (H_2S) is endogenously generated from cysteine by the pyridoxal-5′-phosphate-dependent enzymes, including cystathionine β-synthase (CBS) and cystathionine γ-lyase (CSE). CBS is highly expressed in the brain, whereas CSE is mostly concentrated in the vasculature (10). Homeostasis of H_2S is determined by the balance between generation and degradation of H_2S. Endogenous H_2S can be rapidly oxidized into thiosulfate ($S_2O_3^{2-}$) in the mitochondria, and it is subsequently converted to sulfite (SO_3^{2-}) and sulfate (SO_4^{2-}). H_2S can also be methylated by thiol-*S*-methyltransferase to yield methanethiol (CH_3SH) and dimethylsulfide (CH_3SCH_3). In addition, H_2S has been considered as a powerful reducing agent that can neutralize some endogenous oxidant species such as peroxynitrite, superoxide, and hydrogen peroxide in the vasculature (27).

H_2S has emerged as a new gaseous regulator in the cardiovascular system. Exogenous administration of the H_2S donor, sodium hydrosulfide (NaHS), has been shown to be protective against cardiovascular diseases, such as hypertension (32), ischemia/reperfusion injury (18), myocardial infarction (8), hypertension-induced myocardial hypertrophy (23), and medial thickening of the intramyocardial coronary arterioles (23). H_2S also has been shown to exert other cardiovascular actions, such as an Akt-dependent

Sponsoring Peers: *Jin-Song Bian*, *Samuel Dudley*, *Hideo Kimura and Xian Wang* (see Review Comments in shaded box).

[1]Department of Physiology and Pathophysiology, Fudan University Shanghai Medical College, Shanghai, China.
[2]Department of Radiopharmacy, School of Pharmacy, Fudan University, Shanghai, China.
*These authors contributed equally in this work.

proangiogenic effect (3, 28), protection against cardiomyocyte apoptosis (30), and inhibition of the L-type calcium channels in cardiomyocytes (25).

Moreover, H_2S has been associated with diabetes. An increase in H_2S generation in the pancreas and liver has been observed in a rat model of streptozotocin-induced diabetes (31). In contrast, H_2S biosynthesis has been shown to be decreased in a murine model of type 1 diabetes (15) and a model of nonobese diabetes (2). A more recent study has shown that exogenous administration of an H_2S donor inhibits insulin release in cultured pancreatic β-cells, suggesting that H_2S may impair glucose metabolism and be involved in the pathogenesis of diabetes by an inhibition on insulin release (29). The controversy regarding the role of H_2S in the pathogenesis of diabetes results from the models used (type 1 diabetic models *versus* type 2 diabetic models) and the parameters observed. However, a more clinically relevant question regards a potential role of H_2S in the regulation of insulin receptor (IR) sensitivity and in the development of end-organ damage in type 2 diabetes. This question prompted us to investigate the effects of H_2S on glucose uptake, insulin resistance, and morphological lesions in the kidney of diabetic rats.

Insulin resistance has been shown to have a pivotal role in the pathogenesis of type 2 diabetes, which is characterized by impaired glucose uptake and reduced sensitivity to insulin in major insulin target tissues, such as skeletal muscle, adipose, and liver tissues. Insulin resistance results in an increase in the glucose levels and dysfunction of energy metabolism, which is usually associated with an increase in the insulin levels (20). Increased insulin has been recognized as a growth factor in the induction of pathological processes, such as cardiomyocyte hypertrophy, vascular smooth muscle cell proliferation, and fibroblast proliferation (5). As of yet, however, there is no information about the potential role of H_2S in insulin resistance, glucose uptake, and end-organ damage in diabetes.

On the other hand, the direct target molecules that mediate H_2S actions in various tissues remain unknown. Our previous study has shown that H_2S-induced promotion on angiogenesis is dependent on Akt phosphorylation (3). These data suggest that the target molecules for H_2S exist in the signaling pathways upstream of Akt (including Akt). Interestingly, Akt has been well established as a pivotal signaling element in the signaling pathways downstream of the IR (11). This gives rise to the idea that H_2S may also activate through the signaling pathways upstream of Akt in the insulin target tissues. Therefore, we hypothesize that H_2S may activate insulin signals and promote glucose uptake.

Therefore, the present study had the following aims: to test if H_2S has an insulin-sensitizing effect in type 2 diabetes; to investigate how H_2S regulates the intracellular signals mediated by the IRs; to identify the direct target molecule of H_2S in mediating these effects; and to examine whether a chronic H_2S supplementation may ameliorate kidney damage in type 2 diabetes.

Results

NaHS and H_2S solution promote glucose uptake in myotubes and adipocytes

A decrease in cell viability was observed in myotubes and adipocytes treated with high concentrations (500 and 1000 μM) of the H_2S donor, NaHS (Table 1). Thus, in all

Rebound Track

This work was rejected during a standard peer review and rescued by a Rebound Peer Review (*Antoxid Redox Signal* 16: 293–296, 2012) with the following serving as open reviewers: Jin-Song Bian, Samuel Dudley, Hideo Kimura, and Xian Wang. The comments by these reviewers supporting the rescue are listed below:

Jin-Song Bian (*jinsong_bian@nuhs.edu.sg*): I am a qualified reviewer (per *Antioxid Redox Signal* 16:293–296) and move to rescue this manuscript that was rejected during the regular peer review process after reviewing all versions of the manuscript and detailed reviewer comments. Xue *et al.* found that the treatment with sodium hydrosulfide (NaHS), a hydrogen sulfide (H_2S) donor, increased glucose uptake in both myotubes and adipocytes. More importantly, chronic treatment with NaHS at 30 μmol.kg^{-1}.day^{-1} decreased fasting glucose, increased insulin sensitivity, and increased glucose tolerance in Goto-Kakizaki (GK) diabetic rats. This effect was mediated by activation of the PI3K/Akt/PPAR-gamma pathway. A large amount of evidence was collected to support their findings. Correct methods were employed to examine the effect of H_2S. To my knowledge, this is the first report that chronic treatment with H_2S may potentially serve as an insulin sensitizer for diabetes treatment. The comments from the previous reviewers are sound. I am satisfied with the responses from the authors. Although there is some discrepancy between this and previous reports by Wu *et al.* (*Lab Invest* 89: 59–67, 2009) and by Feng *et al.* (*Biochem Biophys Res Commun* 380: 153–159, 2009), the authors have explained and discussed this discrepancy in the manuscript. In response to the interesting findings of the synergistic effect of endogenous and exogenous H_2S, the authors also proposed a possible mechanism to explain this in the section of Discussion. A more detailed explanation would help the readers better comprehend. Therefore, in the interest of science, I would like to recommend rescuing this work from rejection.

Samuel Dudley (*scdudley@uic.edu*): I am a qualified reviewer (per *Antioxid Redox Signal* 16:293–296) and move to rescue this manuscript that was rejected during the regular peer review process after reviewing all versions of the manuscript and detailed reviewer comments. There is no doubt that the reviewers and the authors have worked hard to improve this article, and that diabetes is a controversial subject that will not be solved with a single manuscript. Clearly, this manuscript raises unanswered questions, including the role of endogenous H_2S, differences with other publications, dissociation of timing between the molecular and physiological changes, certain variances between the *in vivo* and *in vitro* results, the target of H_2S, and the applicability of the potential treatment to various forms of diabetes. I support the publication of these data, because it contributes to debate in an important area, supports a possible mechanism of the H_2S action, has potential translational implications, and is reasonably compressive, if not without controversy. The publication will assist the crucibles of time and colleagues, as they sort out the possibility that H_2S could be a novel treatment for

subsequent experiments, cells were treated with NaHS at concentrations lower than 500 μM.

In myotubes cultured in a medium containing 5.5 mM glucose (without insulin during the culture period, and however, with insulin at 100 nM in the glucose-uptake assay), NaHS treatment for 24 h significantly increased glucose uptake by 1.54 ± 0.21-fold, 1.72 ± 0.22-fold, and 2.06 ± 0.20-fold at concentrations of 25, 50, and 100 μM compared to the control group, respectively (Fig. 1A). NaHS also had a comparable effect in adipocytes, where it increased glucose uptake by 1.47 ± 0.11-fold, 1.73 ± 0.15-fold, and 1.55 ± 0.11-fold at concentrations of 25, 50, and 100 μM in comparison to the control group, respectively (Fig. 1B). Without insulin in the glucose-uptake assay, however, NaHS did not have any effects on glucose uptake in myotubes nor in adipocytes (Table 2).

In myotubes cultured in the presence of insulin (100 nM) and a high level of glucose (25 mM), NaHS also promoted glucose uptake by 1.61 ± 0.16-fold, 1.72 ± 0.14-fold, 1.56 ± 0.10-fold, and 1.46 ± 0.19-fold at concentrations of 25, 50, 100, and 200 μM, respectively (Fig. 1C). Similarly, NaHS promoted glucose uptake by 1.75 ± 0.19-fold, 2.03 ± 0.26-fold, and 1.56 ± 0.14-fold at concentrations of 25, 50, and 100 μM, respectively, in adipocytes cultured in the presence of insulin (100 nM) and a high level of glucose (25 mM) (Fig. 1D). Without insulin in the glucose-uptake assay, however, NaHS did not have any effects on glucose uptake in myotubes nor in adipocytes cultured in a high-glucose (25 mM) medium with insulin (100 nM) (Table 3).

The H_2S gas solution promoted glucose uptake at concentrations of 10, 25, and 50 μM in comparison with the control groups in both myotubes and adipocytes cultured either with low glucose (5.5 mM) (Fig. 1A, B) or with high glucose (25 mM) and insulin (100 nM) (Fig. 1C, D).

We also examined the effects of H_2S on glucose uptake in the presence of insulin at concentrations of 1, 5, 10, and 100 nM. In both myotubes and adipocytes cultured in a low-glucose medium (5.5 mM) (Fig. 1E, F) or in a high-glucose medium (25 mM) (Fig. 1G, H), NaHS treatment (50 μM) for 24 h significantly increased glucose uptake in the presence of insulin at concentrations of 10 and 100 nM; however, NaHS treatment was not effective without insulin or with insulin at concentrations of 1 and 5 nM.

NaHS increases phosphorylation of the IR, PI3K, and Akt

In the presence of low glucose (5.5 mM), NaHS treatment significantly increased IR phosphorylation at concentrations of 25, 50, 100 μM in both myotubes (Fig. 2A) and adipocytes (Fig. 2B). The NaHS-induced (50 μM) increase in IR phosphorylation occurred between 5 and 60 min in myotubes (Fig. 2C) and between 5 and 240 min in adipocytes (Fig. 2D). NaHS treatment also increased PI3K phosphorylation at concentrations of 25, 50, and 100 μM in myotubes (Fig. 3A) and at a concentration of 50 μM in adipocytes (Fig. 3B). NaHS-induced (50 μM) increase in PI3K phosphorylation occurred between 5 and 30 min in myotubes (Fig. 3C) and between 5 and 60 min in adipocytes (Fig. 3D). Similarly, Akt phosphorylation was increased with NaHS treatment at concentrations of 25, 50, and 100 μM in both myotubes (Fig. 4A) and adipocytes (Fig. 4B). The increase in Akt phosphorylation occurred between 5 and

some forms of diabetes and how such a therapy might work. Therefore, in the interest of science, I take the full responsibility to rescue this work from rejection.

Hideo Kimura (*kimura@ncnp.go.jp*): I am a qualified reviewer and move to rescue this manuscript that was rejected during the regular peer review process after reviewing all versions of the manuscript and detailed reviewer comments. This study provided the evidence for the insulin-sensitizing effect of H_2S in the models of insulin resistance both *in vitro* and *in vivo*, and proposed that H_2S treatment may be useful for the therapeutic application to the type 2 diabetes. They showed the following data. H_2S increased glucose uptake in myotubes and adipocytes, and the effects were blocked when the insulin receptors (IRs) and CSE were suppressed by their corresponding siRNAs. Chronic treatment of H_2S increased insulin sensitivity and glucose tolerance, decreased reduced oxygen species levels, and ameliorated diabetic complications in the kidney of the diabetic model animals. These data were appropriately shown, except for two points raised by this reviewer: (i) It is difficult to correctly measure the levels of H_2S in the medium containing serum or in plasma using the H_2S electrodes; (ii) it is not appropriate to use garlic oil as an alternative H_2S donor. Therefore, in the interest of science, I take full responsibility to rescue this work from rejection.

Xian Wang (*xwang@bjmu.edu.cn*): I am a qualified reviewer (per *Antioxid Redox Signal* 16: 293–296) and move to rescue this manuscript that was rejected during the regular peer review process after reviewing all versions of the manuscript and detailed reviewer comments. The potential role of H_2S in diabetes is of significant scientific importance and is attracting, increasing the attention in the field. However, the role of H_2S in diabetes has not been clarified. Despite numerous efforts contributed by scientists in this field, the role of H_2S in diabetes remains controversial. The central question is whether H_2S is beneficial or deleterious in diabetes. It is obvious that both reviewers and authors have worked very hard to improve this study. The authors have properly addressed the concerns raised by the previous reviewers with both new experimental data and appropriate explanation and discussion. To my knowledge, this is the first report that H_2S functions as an insulin sensitizer in type 2 diabetes by using a long-term treatment protocol that have not been used by other investigators. In addition to an amelioration of glucose metabolism, the authors also identified an interesting improvement in the kidney morphology. This study may be advanced to develop new approaches for the treatment of type 2 diabetes. The authors also provided insights into the mechanisms underlying these H_2S actions on glucose metabolism. They identified the IR/PI3K/Akt pathway to mediate the H_2S effects. They also provided evidence to suggest that the IR serves as a direct target for H_2S. The role of endogenous H_2S on the regulation of insulin sensitivity was also investigated. Therefore, this is a comprehensive study on an important topic with significant innovation. In the interest of science, I take the full responsibility to rescue this work from rejection.

Table 1. Effects of Sodium Hydrosulfide Treatment on Cell Viability

	NaHS (μM)							
	0	*10*	*25*	*50*	*100*	*200*	*500*	*1000*
L6 myotubes (% of control)	100.0	98.9±6.3	91.5±7.0	89.0±8.0	86.6±7.5	85.4±7.8	55.1±9.5[a]	43.0±5.2[a]
3T3-L1 adipocytes (% of control)	100.0±3.5	96.9±8.4	93.9±7.2	89.7±9.6	90.9±11.9	81.7±11.9	74.1±1.9[a]	43.7±1.8[a]

[a]$p < 0.05$ *versus* control.
NaHS, sodium hydrosulfide.

120 min in myotubes (Fig. 4C) and between 5 and 60 min in adipocytes (Fig. 4D) after NaHS (50 μM) treatment. NaHS treatment did not affect the total protein levels of the IR, PI3K, and Akt.

NaHS is also effective in increasing phosphorylation of the IR, PI3K, and Akt in the presence of high glucose, and the NaHS effects were blocked with IR inhibition

In the cells cultured with high glucose (25 mM) and insulin (100 nM), NaHS treatment also significantly increased IR phosphorylation at concentrations of 25, 50, 100, and 200 μM in myotubes (Supplementary Fig. S1A; Supplementary Data are available online at www.liebertpub.com/ars) and 25, 50, and 100 μM in adipocytes (Supplementary Fig. S1B). NaHS-induced (50 μM) increase in IR phosphorylation occurred at 15, 30, and 60 min in myotubes (Supplementary Fig. S1C) and at 15, 30, 60, 120, and 240 min in adipocytes (Supplementary Fig. S1D). NaHS treatment also increased PI3K phosphorylation at concentrations of 50 and 100 μM in myotubes (Supplementary Fig. S2A) and at concentrations of 25, 50, and 100 μM in adipocytes (Supplementary Fig. S2B). NaHS-induced (50 μM) increase in PI3K phosphorylation occurred at 30, 60, and 120 min in myotubes (Supplementary Fig. S2C) and at 15, 30, 60, 120, and 240 min in adipocytes (Supplementary Fig. S2D). Similarly, Akt phosphorylation was increased with NaHS treatment at concentrations of 50, 100, and 200 μM in myotubes (Supplementary Fig. S3A) and 50 and 100 μM in adipocytes (Supplementary Fig. S3B). The increase in Akt phosphorylation occurred between 5 and 60 min in myotubes (Supplementary Fig. S3C) and between 15 and 120 min in adipocytes (Supplementary Fig. S3D) after NaHS (50 μM) treatment. NaHS treatment did not change the total protein levels of the IR, PI3K, or Akt (Supplementary Figs. S1–S3). In the absence of NaHS, a high-glucose (25 mM) culture with insulin (100 nM) decreased phosphorylation of the IR in both myotubes (Supplementary Fig. S4A) and adipocytes (Supplementary Fig. S4B) as compared with that of the cells with the low-glucose culture (5.5 mM). PI3K phosphorylation was also decreased either in myotubes (Supplementary Fig. S5A) or in adipocytes (Supplementary Fig. S5B) cultured with high glucose (25 mM) with insulin (100 nM) as compared with that of the cells cultured with low glucose (5.5 mM) in absence of NaHS (50 μM). Similarly, a high-glucose (25 mM) culture with insulin (100 nM) decreased Akt phosphorylation in myotubes (Supplementary Fig. S5C) and in adipocytes (Supplementary Fig. S5D) as compared with that cultured with low glucose (5.5 mM) in the absence of NaHS (50 μM).

The NaHS-induced increase in the phosphorylation of both the IR (Supplementary Fig. S6A, B) and PI3K (Supplementary Fig. S7A, S7B) was prevented by the IR inhibitor, HNMPA, in both myotubes and adipocytes. The effect of NaHS on Akt phosphorylation was also prevented by HNMPA in myotubes (Supplementary Fig. S7C), however, was not blunted by HNMPA in the adipocytes (Supplementary Fig. S7D).

The effects of NaHS in increasing glucose uptake were inhibited in the cells pretreated with a PI3K inhibitor or an IR inhibitor

An NaHS-induced increase in glucose uptake in both myotubes and adipocytes was abolished by coadministration of the IR inhibitor, HNMPA (300 μM), or the PI3K inhibitor, LY294002 (5 μM), in the presence of low level (5.5 mM) of glucose (Fig. 5A, B), suggesting a role of the IR/PI3K pathway in the mediation of these NaHS effects.

The effects of NaHS in increasing glucose uptake were inhibited in the cells with siRNA-mediated knockdown of the IR

siRNA-mediated knockdown of the IR was induced either in myotubes or in adipocytes, and the control cells were transfected with vectors. The expression of the IR protein was decreased by 45.87% in myotubes cultured with low glucose (5.5 mM) (Fig. 5C), by 38.05% in myotubes cultured with high glucose (25 mM) and insulin (100 nM) (Fig. 5E), by 51.25% in adipocytes cultured with low glucose (5.5 mM) (Fig. 5D), and by 41.46% in adipocytes cultured with high glucose (25 mM) and insulin (100 nM) (Fig. 5F) in 48 h after transfection with siRNA against the IR.

The effects of NaHS in increasing glucose uptake were inhibited in either myotubes (Fig. 5C, E) or adipocytes (Fig. 5D, F) with IR knockdown in the presence of low glucose (5.5 mM) (Fig. 5C, D) or high glucose (25 mM) with insulin (100 nM) (Fig. 5E, F). These data indicate that the NaHS effects in promoting glucose uptake are dependent on the IRs.

NaHS directly activates the IR in a cell-free system

To further examine if the IR was a direct target molecule of H_2S, a pure recombinant IR protein was allowed to react with NaHS for 1 h in a cell-free system without any other cellular elements. As shown in Figure 5G, NaHS significantly increased the kinase activity of the IR at concentrations of 50 and 400 μM.

NaHS did not inhibit the enzyme activity of protein tyrosine phosphatase 1B

To further clarify the mechanisms of NaHS-induced phosphorylation of the protein kinases, the activity of protein tyrosine phosphatase 1B (PTP1B) was measured using a commercial kit. The results showed that the activity of PTP1B was not inhibited, but increased after treatment with NaHS at concentrations of 1–400 μM as compared with a vehicle-treated control (Fig. 5H).

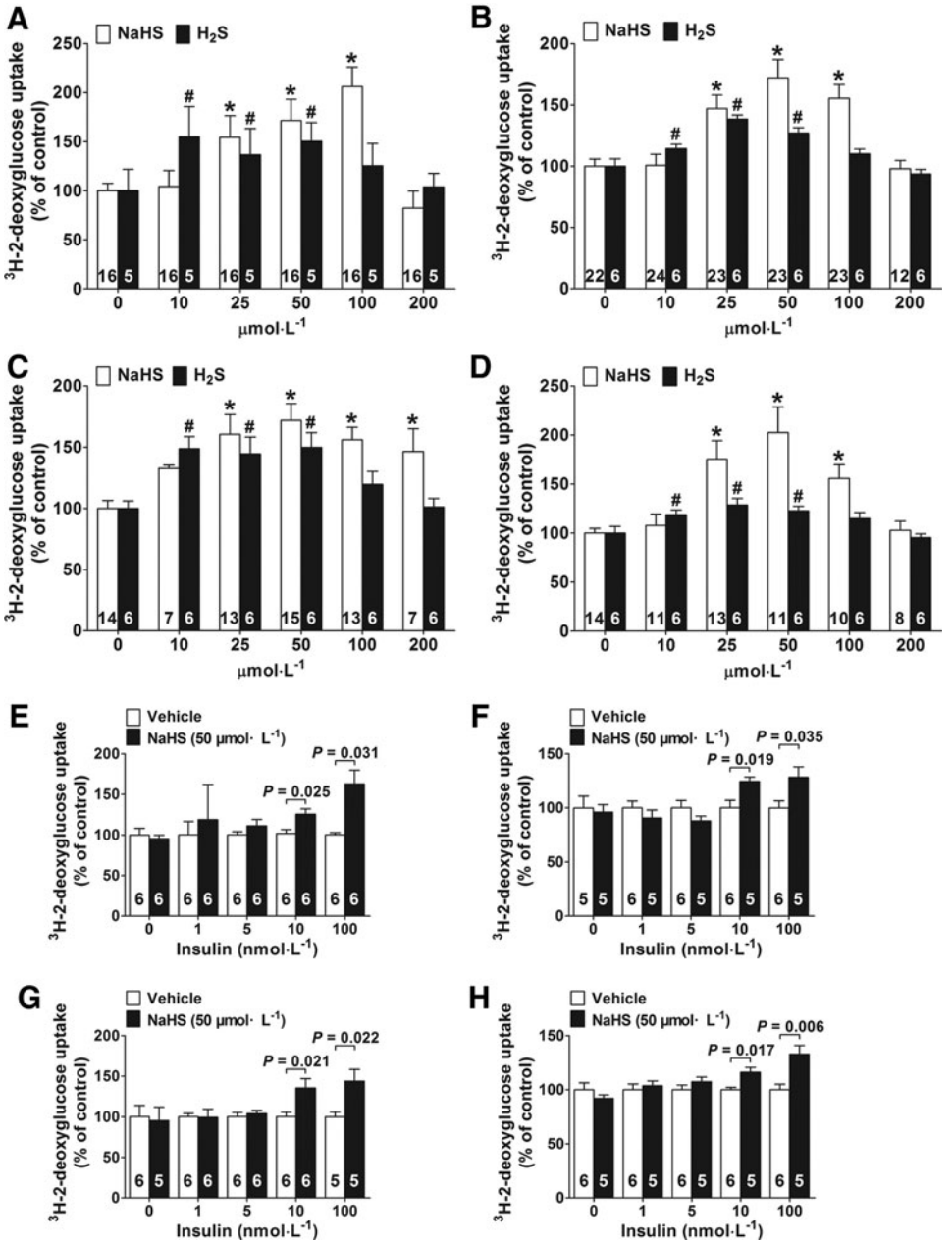

FIG. 1. Effects of H_2S treatment on 2-deoxyglucose uptake in L6 myotubes and 3T3-L1 adipocytes. Exogenous administration of H_2S was applied by administering the H_2S donor, NaHS, and H_2S solution for 24 h. The effects of NaHS and H_2S solution on 2-deoxyglucose uptake in L6 myotubes **(A)** and 3T3-L1 adipocytes **(B)** cultured in a low-glucose medium (5.5 m*M*). The effects of NaHS and H_2S gas solution on 2-deoxyglucose uptake in L6 myotubes **(C)** and 3T3-L1 adipocytes **(D)** cultured in a high-glucose medium (25 m*M*) with insulin (100 n*M*). $^*p < 0.05$ *vs.* NaHS control (NaHS = 0 μM) for **(A–D)**; $^\#p < 0.05$ *vs.* H_2S control ($H_2S = 0\ \mu M$) for **(A–D)**; **(E–H)** effect of H_2S (50 μM) on 2-deoxyglucose uptake in the absence or presence of insulin at different concentrations (1, 5, 10, and 100 n*M*) during the cell culture period and also in the glucose uptake assay. **(E, F)** At concentrations of 50 μM, NaHS treatment significantly increases 2-deoxyglucose uptake in L6 myotubes and 3T3-L1 adipocytes cultured in a low-glucose medium (5.5 m*M*) at an insulin concentration of 10 and 100 n*M*. **(G, H)** NaHS treatment (50 μM) significantly promotes 2-deoxyglucose uptake in L6 myotubes and 3T3-L1 adipocytes cultured in a high-glucose medium (25 m*M*) at an insulin concentration of 10 and 100 n*M*. Data represent means ± SE. A p value < 0.05 represents statistical significance. NaHS, sodium hydrosulfide; SE, standard error.

Comparison of the promoting effects of NaHS on glucose uptake with some thiol compounds in myotubes and adipocytes

Effects of several biological thiols on the regulation of glucose uptake were also examined in both myotubes and adipocytes. In myotubes, glutathione (GSH) increased glucose uptake at concentrations of 25, 50, 100, and 200 μM in a low-glucose (5.5 m*M*) medium (Supplementary Fig. S10A). In adipocytes, GSH increased glucose uptake at concentrations of 25 and 100 μM in a low-glucose (5.5 m*M*) medium (Supplementary Fig. S10B). However, GSH was less effective in

Table 2. Effects of Sodium Hydrosulfide Treatment on ^{3}H-2-Deoxyglucose Uptake Cultured with 5.5 m*M* Glucose in the Absence of Insulin

	NaHS (μM)					
	0	*10*	*25*	*50*	*100*	*200*
^{3}H-2-deoxyglucose uptake in L6 myotubes (% of control)	100.0 ± 14.7	90.1 ± 13.5	85.0 ± 7.1	106.5 ± 17.3	115.8 ± 12.6	87.4 ± 12.2
^{3}H-2-deoxyglucose uptake in 3T3-L1 adipocytes(% of control)	100.0 ± 3.8	94.8 ± 5.3	114.4 ± 12.8	88.5 ± 11.8	93.5 ± 9.8	73.7 ± 5.14

myotubes cultured in a high-glucose (25 m*M*) medium with insulin (100 n*M*) than NaHS at a concentration of 25 μM (Supplementary Fig. S10C). L-cysteine only promotes glucose uptake at concentrations of 25 and 50 μM in myotubes cultured in a high-glucose (25 m*M*) medium with insulin (100 n*M*) (Supplementary Fig. S10C). L-cysteine showed no effect in myotubes and adipocytes cultured in a low-glucose (5.5 m*M*) medium (Supplementary Fig. S10A, B). In contrast, L-cysteine caused a decrease in glucose uptake at concentrations of 25, 50, and 100 μM in adipocytes cultured with high glucose (25 m*M*) and insulin (100 n*M*) (Supplementary Fig. S10D).

Glucose uptake was decreased in the cells with siRNA-mediated knockdown of CSE

To examine the role of endogenous H_2S in the regulation of cellular glucose uptake, siRNA-mediated CSE silencing was induced either in myotubes or in adipocytes. CSE protein levels were decreased by 60.74% in myotubes cultured with low glucose (5.5 m*M*) (Fig. 6A), by 59.29% in myotubes cultured with high glucose (25 m*M*) and insulin (100 n*M*) (Fig. 6C), by 43.63% in adipocytes cultured with low glucose (5.5 m*M*) (Fig. 6B), and by 35.75% in adipocytes cultured with high glucose (25 m*M*) and insulin (100 n*M*) (Fig. 6D) in 48 h after transfection with siRNA against CSE.

In basal conditions without exogenous H_2S, CSE knockdown only caused a decrease in glucose uptake in adipocytes cultured with low glucose (5.5 m*M*) (Fig. 6B). Interestingly, in the presence of exogenous H_2S, CSE knockdown exerted a significant inhibition on glucose uptake in both myotubes (Fig. 6A, C) and adipocytes (Fig. 6B, D) in the presence of either low glucose (5.5 m*M*) (Fig. 6A, B) or high glucose (25 m*M*) with insulin (100 n*M*) (Fig. 6C, D). The data suggest that endogenous H_2S generated from CSE has a role in the regulation of glucose uptake under certain basal conditions or in the presence of a certain concentration of exogenous H_2S.

NaHS does not affect the phosphorylation of c-Cbl, ERK, p38, or c-JNK

NaHS (50 μM) treatment for 60 min did not change the phosphorylation levels of c-Cbl (Supplementary Fig. S8A, B), ERK (Supplementary Fig. S8C, D), p38 (Supplementary Fig. S9A, B), or JNK (Supplementary Fig. S9C, D) in myotubes or in adipocytes cultured in a low-glucose (5.5 m*M*) medium.

These *in vitro* experiments suggested that NaHS sensitized the IR and activated the PI3K/Akt signaling pathway. The *in vivo* effects of H_2S on glucose metabolism, insulin sensitivity, and kidney morphology were further examined in Goto-Kakizaki (GK) diabetic rats and Wistar rats with a chronic treatment of NaHS.

Chronic NaHS treatment increases insulin sensitivity and changes glucose tolerance in both GK and Wistar rats

Insulin sensitivity tests demonstrated that insulin injection caused a more significant decrease in plasma glucose levels in GK rats treated with NaHS for 10 weeks at a dose of 30 $\mu mol \cdot kg^{-1} \cdot day^{-1}$ as compared to the GK control (Fig. 7A). In Wistar rats, chronic treatment with NaHS increased insulin sensitivity at a dose of 60 $\mu mol \cdot kg^{-1} \cdot day^{-1}$ (Fig. 7B). In insulin sensitivity tests using a lower insulin concentration (0.4 $U \cdot kg^{-1}$) and a short starvation time (4 h), the insulin-sensitizing effects were more pronounced in Wistar rats treated with NaHS at a dose of 60 $\mu mol \cdot kg^{-1} \cdot day^{-1}$ as compared with the vehicle-treated Wistar control group (Fig. 7C).

During the treatment period of 10 weeks, fasting plasma glucose was decreased in GK rats treated with NaHS at a dose of 30 $\mu mol \cdot kg^{-1} \cdot day^{-1}$ in 4, 6, 8, and 10 weeks. In contrast, NaHS treatment at a high dose of 120 $\mu mol \cdot kg^{-1} \cdot day^{-1}$ caused a transient increase in fasting plasma glucose in 6 weeks (Fig. 7D). In Wistar rats treated with NaHS at 60 $\mu mol \cdot kg^{-1} \cdot day^{-1}$, the fasting plasma glucose levels were significantly decreased as compared with that of the Wistar

Table 3. Effects of Sodium Hydrosulfide Treatment on ^{3}H-2-Deoxyglucose Uptake Cultured with 25 m*M* Glucose in the Absence of Insulin

	NaHS (μM)					
	0	*10*	*25*	*50*	*100*	*200*
^{3}H-2-deoxyglucose uptake in L6 myotubes (% of control)	100.0 ± 25.67	93 ± 8.23	84.1 ± 5.09	88.3 ± 7.97	105.7 ± 14.72	75.7 ± 6.58
^{3}H-2-deoxyglucose uptake in 3T3-L1 adipocytes (% of control)	100.0 ± 12.18	95.3 ± 5.58	80.3 ± 10.88	98.4 ± 15.99	84.2 ± 15.70	83.8 ± 8.50

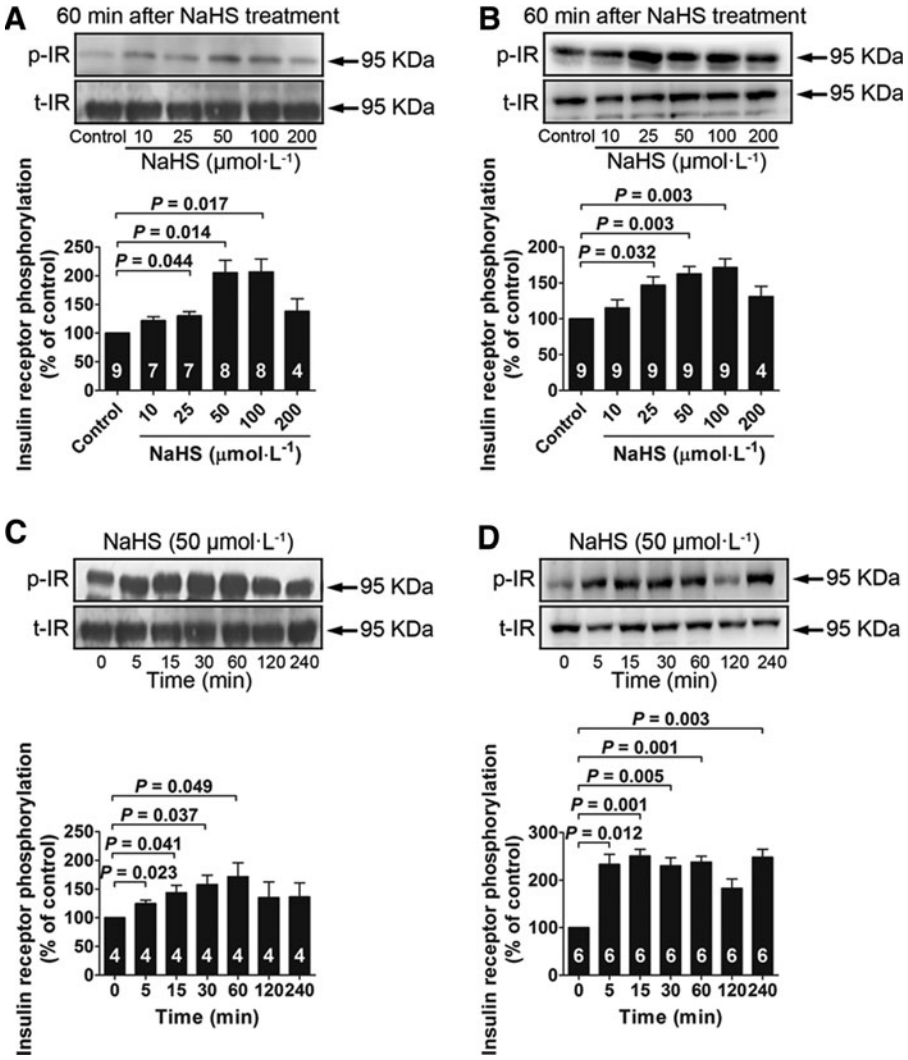

FIG. 2. NaHS treatment increases IR phosphorylation in L6 myotubes and 3T3-L1 adipocytes. (A, B) Dose–response of NaHS treatment (10–200 μM) for 60 min on phosphorylation of the IR in L6 myotubes and 3T3-L1 adipocytes cultured in a low-glucose medium (5.5 mM). **(C, D)** Time course of phosphorylation induced by NaHS (50 μM) in L6 myotubes and 3T3-L1 adipocytes cultured in a low-glucose medium (5.5 mM). Data represent means ± SE. A p value < 0.05 represents statistical significance. H_2S, hydrogen sulfide; IR, insulin receptor.

control group in 4, 6, 8, and 10 weeks during the treatment period (Fig. 7D). Similarly, in the Wistar rats treated with NaHS at 30 $\mu mol \cdot kg^{-1} \cdot day^{-1}$, the fasting plasma glucose levels were significantly decreased as compared with that of the Wistar control group in 4, 6, and 8 weeks during the treatment period (Fig. 7D). Moreover, in the Wistar rats treated with NaHS at 120 $\mu mol \cdot kg^{-1} \cdot day^{-1}$, the fasting plasma glucose levels were transiently decreased as compared with that of the Wistar control group at an 8-week treatment time (Fig. 7D). At the end of the 10-week treatment period, the fasting plasma insulin levels were significantly decreased in all groups of GK rats as compared to the plasma insulin levels in Wistar control rats (Fig. 7H).

A glucose tolerance test (GTT) was performed 2 weeks before the end of the 10-week treatment period. The GK rats treated with NaHS at a dose of 30 $\mu mol \cdot kg^{-1} \cdot day^{-1}$ had an increase in glucose tolerance in which the plasma glucose levels were significantly lower than that of the GK control group at 0, 30, and 90 min of the test period (Fig. 7E). In Wistar rats, treatment with NaHS at a dose of 60 $\mu mol \cdot kg^{-1} \cdot day^{-1}$ significantly decreased the plasma glucose levels at 0, 30, and 60 min, whereas treatment with NaHS at a dose of 30 $\mu mol \cdot kg^{-1} \cdot day^{-1}$ significantly decreased the plasma glucose levels at 30 min during the test period as compared to the Wistar control group (Fig. 7F). The area under curve (AUC) of glucose levels of GK rats treated with NaHS at a dose of 30 $\mu mol \cdot kg^{-1} \cdot day^{-1}$ was significantly decreased as compared with that of the GK control rats (Fig. 7G). On the other hand, the AUC of glucose levels in the GK control group was significantly increased as compared with that of the Wistar control group, suggesting that the GK rats have a decreased glucose tolerance than the Wistar rats (Fig. 7G). In addition, the plasma insulin levels measured at some time points during the GTT were increased in GK rats treated with NaHS (Fig. 7I). There was no sustained increase in the insulin levels in Wistar rats treated with NaHS during the period of GTT (Fig. 7J).

To examine whether the blood glucose assay values would be influenced by the potential reducing property of NaHS, plasma was collected from five starved rats, and each sample was divided into two paired samples with the same volume that applied with vehicle or NaHS (30 μM), and then glucose levels were measured with these samples. The results showed that the glucose values are almost identical in these pairs of samples, and the statistical analysis showed that there is no significant difference between the two groups (Supplementary Fig. S11C). Therefore, it can be concluded that NaHS (30 μM) contained in the plasma samples does not affect the

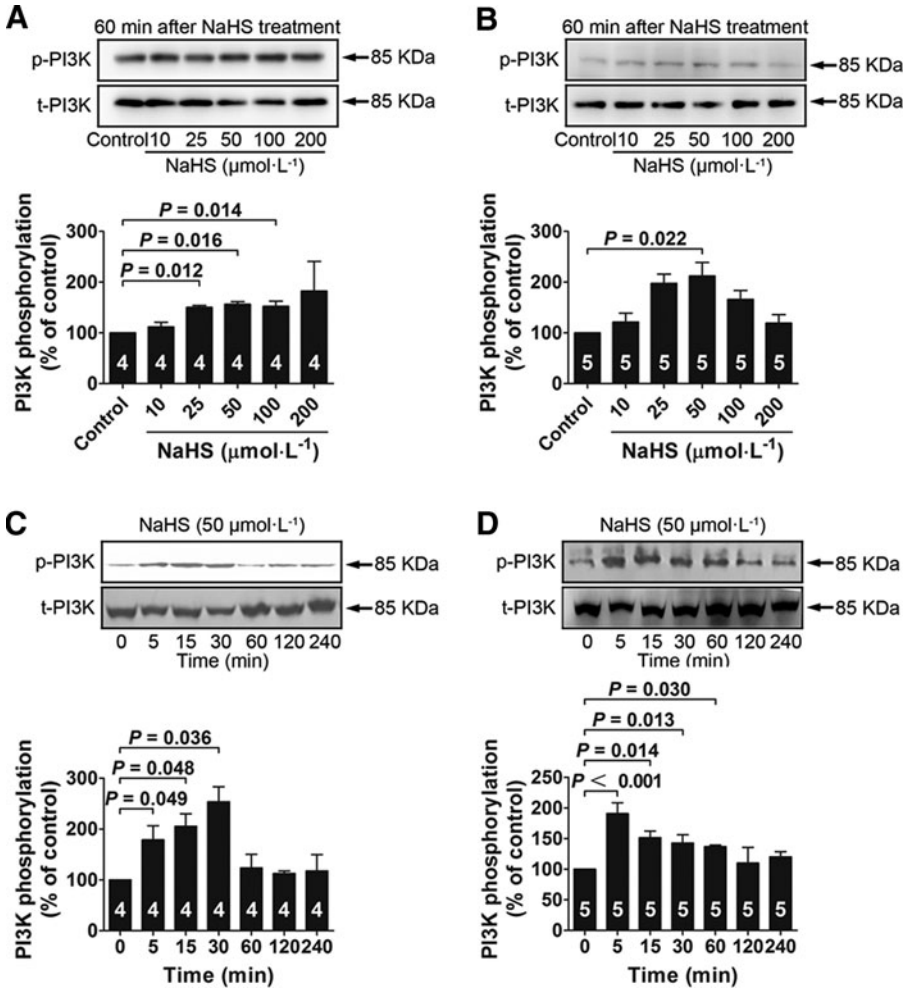

FIG. 3. NaHS treatment increases PI3K phosphorylation in L6 myotubes and 3T3-L1 adipocytes. **(A, B)** Effects of a 60-min treatment with various concentrations of NaHS (10–200 μM) on PI3K phosphorylation in L6 myotubes and 3T3-L1 adipocytes cultured in a low-glucose medium (5.5 mM). **(C, D)** Time course of PI3K phosphorylation induced by NaHS (50 μM) in L6 myotubes and 3T3-L1 adipocytes cultured in a low-glucose medium (5.5 mM). Data represent means ± SE. A p value < 0.05 represents statistical significance.

values of plasma glucose measured with the methods used in the present study.

Chronic NaHS treatment reduced reduced oxygen species levels in the kidney of GK rats

Reduced oxygen species (ROS) expression in the kidney was examined in the kidney at the end of the 10-week treatment period. The results showed that the ROS levels in the kidney in GK control rats was increased as compared with that of Wistar control rats. Chronic H_2S treatment caused a significant decrease in ROS expression in the kidney of GK rats treated with NaHS at concentrations of 30, 60, and 120 $\mu mol \cdot kg^{-1} \cdot day^{-1}$ as compared with that of GK control rats treated with vehicle (Fig. 8A, C).

Number of the crescentic glomeruli was decreased in the kidney of GK rats chronically treated with NaHS

There is no sign of glomerular fibrosis, including Kimmelstiel-Wilson nodules, in the kidney of GK rats (Fig. 8B). The obvious morphological change was an increase in the number of crescentic glomeruli observed in the kidney of GK rats (Fig. 8B, D). The number of crescentic glomeruli was decreased in the kidney of GK rats chronically treated with NaHS at doses of 30, 60, and 120 $\mu mol \cdot kg^{-1} \cdot day^{-1}$ (Fig. 8B, D).

The effect of chronic NaHS treatment on GSH and the ratio of GSH to GSSG in GK rats

GSH and the ratio of GSH to oxidized GSH (GSSG) were decreased in the liver of GK rats as compared to that of the Wistar rats (Supplementary Fig. S11A, B). Chronic NaHS treatment for 10 weeks caused an increase in GSH levels at doses of 60 and 120 $\mu mol \cdot kg^{-1} \cdot day^{-1}$ (Supplementary Fig. S11A) and an increase in the ratio of GSH to GSSG at a dose of 120 $\mu mol \cdot kg^{-1} \cdot day^{-1}$ (Supplementary Fig. S11B) as compared with that of the GK control group.

Chronic NaHS treatment reduces plasma cholesterol levels and blood pressure in GK diabetic rats and Wistar rats

As shown in Table 4, high density lipoprotein (HDL) cholesterol was increased, but fasting glucose, total cholesterol, low-density lipoprotein (LDL) cholesterol and blood pressure were significantly reduced with NaHS treatment at a dose of 30 $\mu mol \cdot kg^{-1} \cdot day^{-1}$ for 6 weeks in GK rats. At the dose of 60 $\mu mol \cdot kg^{-1} \cdot day^{-1}$, total cholesterol and blood pressure were also decreased with NaHS treatment. At the high dose of 120 $\mu mol \cdot kg^{-1} \cdot day^{-1}$, the increase in HDL cholesterol was still observed, but fasting plasma glucose was increased.

In Wistar rats, chronic NaHS treatment for 6 weeks caused an increase in HDL cholesterol and a decrease in total

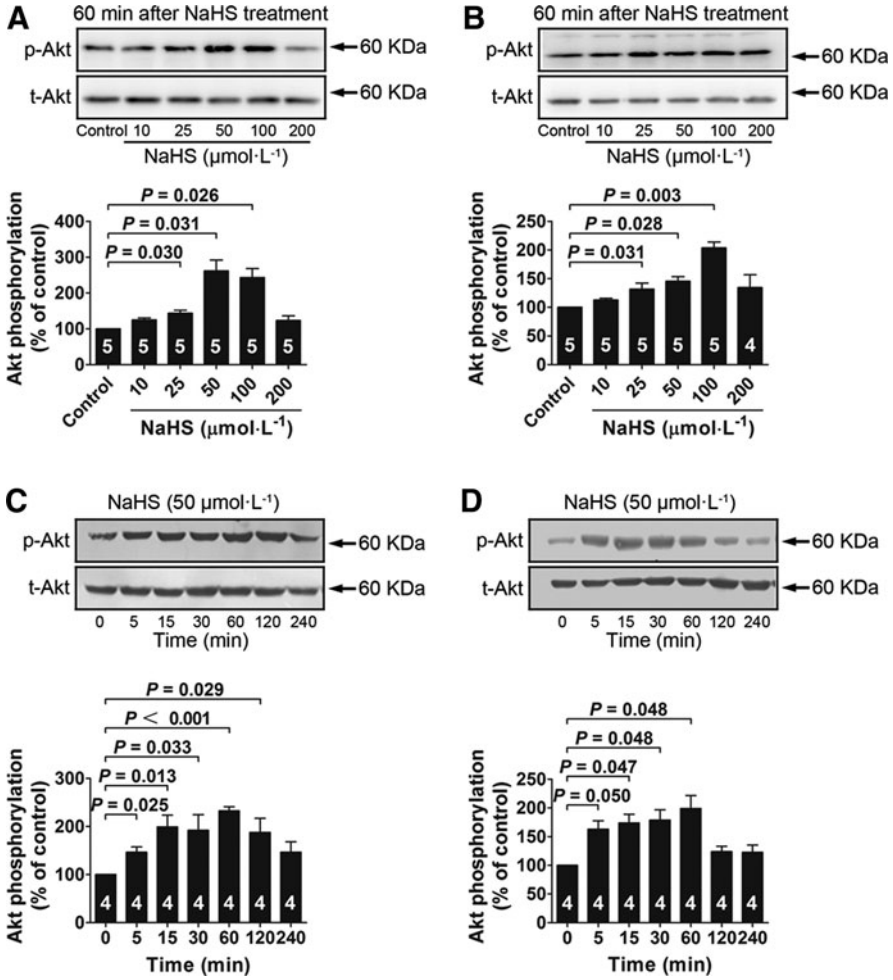

FIG. 4. NaHS treatment increases Akt phosphorylation in L6 myotubes and 3T3-L1 adipocytes with insulin (100 n*M*) stimulation. (A, B) Effects of a 60-min treatment with various concentrations of NaHS (10–200 μM) on Akt phosphorylation in L6 myotubes and 3T3-L1 adipocytes cultured in a low-glucose medium (5.5 m*M*). **(C, D)** Time course of Akt phosphorylation induced by NaHS (50 μM) in L6 myotubes and 3T3-L1 adipocytes cultured in a low-glucose medium (5.5 m*M*). Data represent means ± SE. A p value < 0.05 represents statistical significance.

cholesterol and triglycerides (TG) at a dose of 30 μmol·kg^{-1}·day^{-1}. At the high dose of 120 μmol·kg^{-1}·day^{-1}, NaHS treatment also caused an increase in HDL cholesterol (Table 5).

Effect of NaHS treatment on PI3K and Akt phosphorylation in GK rats

The expression and phosphorylation levels of several signaling elements were examined by the Western blot analysis in muscle and fat tissues from GK rats at the end of the 10-week NaHS treatment. In the muscle tissue, PI3K and Akt phosphorylation was increased with NaHS treatment at the dosage of 30 μmol·kg^{-1}·day^{-1}, but not at dosages of 60 and 120 μmol·kg^{-1}·day^{-1} (Fig. 9A, C). In the abdominal fat tissue, PI3K and Akt phosphorylation was not changed with NaHS treatment (Fig. 9B, D).

Discussion

Type 2 diabetes is characterized by impaired utilization of glucose in tissues, leading to an increase in circulating glucose and insulin resistance. A major approach in treating type 2 diabetes is to recover insulin resistance by using insulin-sensitizing drugs (17). On the other hand, the mechanisms underlying insulin resistance remain to be further clarified.

The present study suggests that NaHS treatment may ameliorate insulin resistance by sensitizing IR-mediated signals. In contrast to our findings, a decrease in glucose uptake has been found in rat adipocytes 30 min after H_2S treatment (4). This discrepancy may be due to the difference in the time points examined and cell origin. In the present study, the glucose uptake was measured 24 h after NaHS treatment. NaHS needs to trigger a cascade of intracellular signaling events that result in an increase in glucose uptake. These signaling events may take several hours to finally affect the glucose uptake property of the cells. Thirty minutes may be too early to examine the NaHS-induced increase in glucose uptake.

The signaling mechanisms underlying NaHS-induced insulin sensitization were further investigated in the present study. IRs are receptor tyrosine kinases that are activated by *trans*-autophosphorylation upon insulin binding to their extracellular domains (22, 21). Subsequently, IR substrate-1 is phosphorylated at the tyrosine sites and then binds to PI3K, which activates Akt (11). In this study, we showed that phosphorylation of the IR, PI3K, and Akt was increased in myotubes and adipocytes treated with NaHS. However, the ability of NaHS to activate PI3K was blocked by the IR inhibitor HNMPA. Moreover, NaHS directly activated the IRs in a cell-free system, suggesting that the IR may function as a direct target molecule for NaHS, and that PI3K serves as an element downstream of the IRs in NaHS actions. This idea was further supported by the experiments where the NaHS-induced increase in glucose uptake was prevented by siRNA-mediated knockdown of the IR, or by

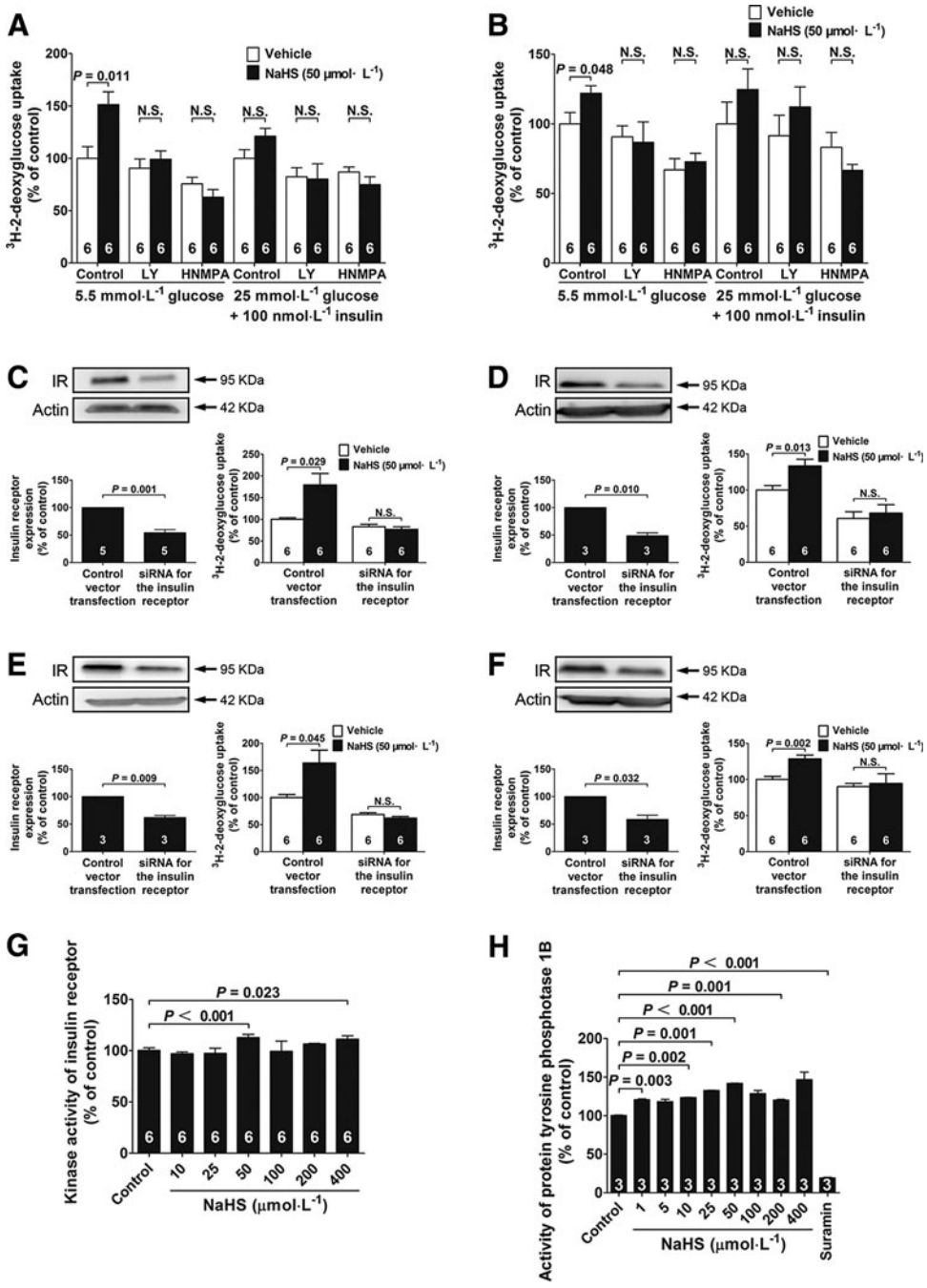

FIG. 5. The role of the insulin receptor in NaHS-induced increase in glucose uptake. Effects of the PI3K inhibitor LY 294002 and the IR inhibitor HNMPA on NaHS-induced glucose uptake in L6 myotubes **(A)** and 3T3-L1 adipocytes **(B)**. Western blot analysis of the expression of the IR in myotubes **(C)** and adipocytes **(D)** cultured in a low-glucose medium (5.5 m*M*) after transfection with siRNA against the IR. NaHS-induced increase in glucose uptake is blunted in myotubes **(C)** and adipocytes **(D)** with siRNA-mediated knockdown of the IR in the presence of low glucose (5.5 m*M*). **(E, F)** Western blot analysis of the expression of the IR in myotubes **(E)** and adipocytes **(F)** cultured in a high-glucose medium (25 m*M*) with insulin (100 n*M*) after transfection with siRNA against the IR. NaHS-induced increase in glucose uptake is blunted in myotubes **(E)** and adipocytes **(F)** with siRNA-mediated knockdown of the IR in the cells cultured with high glucose (25 m*M*) and insulin (100 n*M*). **(G)** NaHS directly activates the IR in a cell-free system. **(H)** Effects of NaHS (10–400 μM) on PTP1B enzyme activity. Suramin (10uM) was added as a positive control of PTP1B inhibition. Data represent means ± SE. A p value < 0.05 represents statistical significance. PTP1B, protein tyrosine phosphatase 1B.

pretreatment with the IR inhibitor, HNMPA, or the PI3K inhibitor, LY294002. Indeed, the increase in the IR kinase activity with NaHS treatment in a cell-free system is only about 10%, which may hardly affect signaling. It is possible that the conformation and function of the IR in the cell-free system may not be identical with those in the living cells where some elements interacting with the receptor are present. If the IR functions as direct target molecules for H_2S in living cells, the increase in kinase activity of the IR may be more pronounced in living cells due to conformational changes and some possible interaction with other cellular elements. As of yet, there is no evidence about the direct target molecule for H_2S to mediate important physiological functions in the insulin-targeting cells. Whether the IR functions as a direct target molecule for H_2S remains to be further clarified.

On the other hand, the IR inhibitor prevented NaHS-induced Akt phosphorylation in myotubes, but not in adipocytes. The role of Akt in mediating the NaHS actions on glucose metabolism may be tissue dependent.

It is unknown how NaHS interacts with the IR and how this interaction can activate the receptor. NaHS may react with some amino acid residues of the IR, resulting in certain chemical modifications of the residues and subsequent changes in the conformation of the IRs. These conformational changes induced by NaHS may promote *trans*-autophosphorylation of IRs and thus increase receptor activation. This hypothesis remains to be investigated in future studies.

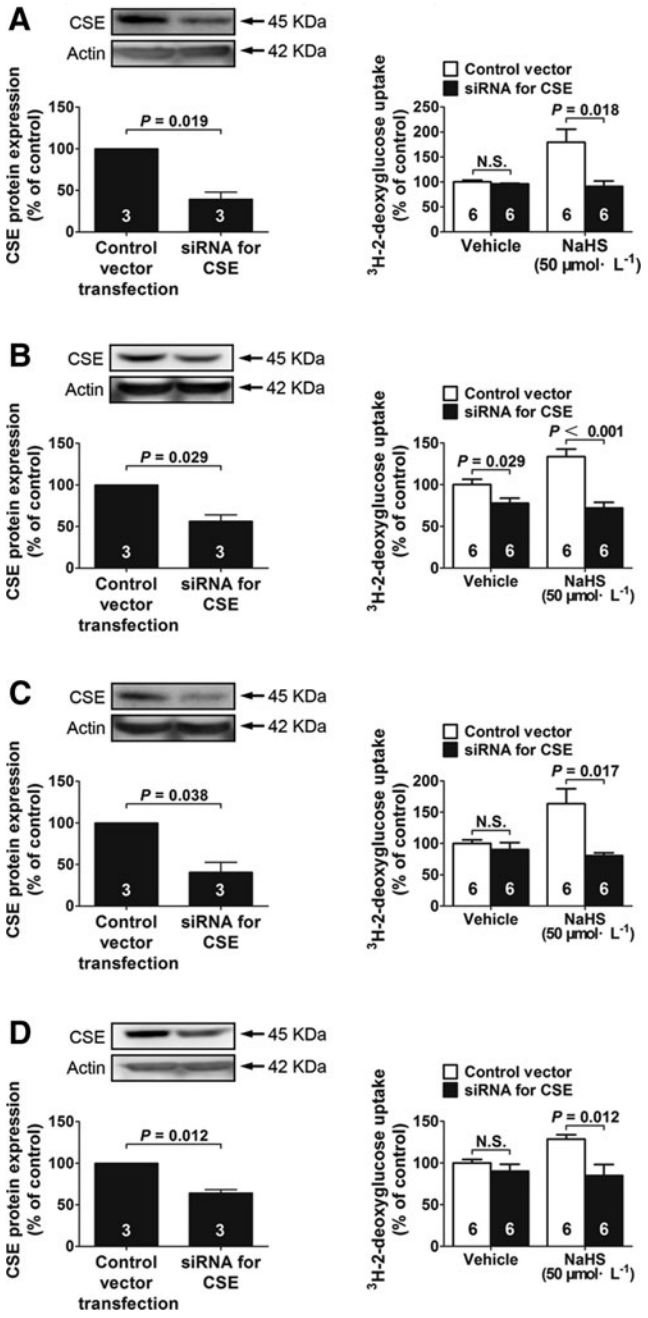

FIG. 6. The role of endogenous H_2S in the regulation of glucose uptake in both myotubes and adipocytes. (A, B) Effects of siRNA-mediated knockdown of CSE on CSE expression and glucose uptake in myotubes **(A)** and adipocytes **(B)** cultured in a low-glucose medium (5.5 m*M*) in the absence or presence of NaHS (50 μM). Effects of siRNA-mediated knockdown of CSE on CSE expression and glucose uptake in myotubes **(C)** and adipocytes **(D)** cultured in a high-glucose medium (25 m*M*) with insulin (100 n*M*) in the absence or presence of NaHS (50 μM). Data represent means ± SE. A p value < 0.05 represents statistical significance. CSE, cystathionine γ-lyase.

It is worthy of notice that NaHS increased glucose uptake in 24 h after treatment, whereas the maximum time of phosphorylation of the IR/PI3K/Akt by NaHS is about 4 h. We have observed similar long-lasting effects of H_2S treatment on promoting migration and tube formation of vascular endothelial cells in 16–24 h, whereas the increase in Akt phosphorylation lasts < 2 h (3). Indeed, our present data are not sufficient to clarify the whole signaling cascade that mediates the promoting effects of NaHS treatment on glucose uptake. The IR/PI3K/Akt activation may function as an early event for the whole cascade of signaling events triggered by NaHS. It may take a much longer time to go through all the signaling pathways that finally result in an increase in glucose uptake.

In addition, the insulin signals are negatively regulated by PTPs among which PTP1B has been considered as a key regulator for the IR (6). In the present study, we did not observe an inhibition of PTP1B in the presence of NaHS. In fact, the PTP1B activity was increased in the presence of NaHS. This result does not suggest a potential role of PTP1B in mediating an NaHS-induced increase in the phosphorylation of the IRs.

Additional pathways have been reported to mediate the signals downstream of the IRs. For example, insulin stimulates GLUT4 translocation and glucose uptake by phosphorylation of the adaptor protein, c-Cbl (24). However, this pathway may not be important in mediating the NaHS effects in the present study, because Cbl phosphorylation was not changed with NaHS treatment. Another pathway downstream of the IRs is the MAPK pathway (13). Similarly, this pathway did not have a role in mediating the NaHS effects in the present study, because the MAPK-signaling molecules, including ERK, p38, and JNK, were not activated by NaHS.

The stimulating effects of NaHS on the IRs may have a potential clinical relevance. This idea was supported by the *in vivo* experiments where GK diabetic rats were chronically treated with an H_2S donor for 10 weeks. Insulin sensitivity was increased in the GK rats treated with NaHS at a dose of 30 μmol·kg^{-1}·day^{-1}. Moreover, fasting blood glucose levels were decreased, and glucose tolerance was increased in GK rats chronically treated with NaHS at a dose of 30 μmol·kg^{-1}·day^{-1}. Activation of the PI3K/Akt pathway was also observed in some of the tissues in the GK rats treated with NaHS. This is in line with the *in vitro* experiments. It has been shown that H_2S inhibits insulin secretion in freshly isolated rat pancreatic β-cells (29). In the present study, however, the plasma insulin levels were also increased after a 10-week NaHS treatment in the GK diabetic rats. This suggests that NaHS treatment also has an effect on insulin biosynthesis, and this effect may also contribute to the amelioration observed in GK rats. We found here that chronic NaHS treatment also increased insulin sensitivity and reduced plasma fasting glucose levels at dosage of 30 and 60 μmol·kg^{-1}·day^{-1} in Wistar rats. These data further confirm that the insulin-sensitizing effects of exogenous H_2S treatment are also present in the subjects without diabetes.

In contrast, the dose of NaHS at 120 μmol·kg^{-1}·day^{-1} did not exert an insulin-sensitizing effect in GK rats nor in Wistar rats. The mechanisms underlying these effects are unknown. NaHS may act on multiple types of cells, and crosstalks of different H_2S signals on glucose metabolism based on a cell–cell interaction mechanism may be involved. H_2S may activate some mechanisms inhibitory to the insulin signals at higher doses such as 120 μM NaHS, while these purported inhibitory pathways are only present in *in vivo* models. In contrary, a decrease in blood glucose is observed in Zucker diabetic rats treated with a CSE inhibitor, DL-propargylglycine (PPG), for 4 weeks (29). This discrepancy may be due to the difference in

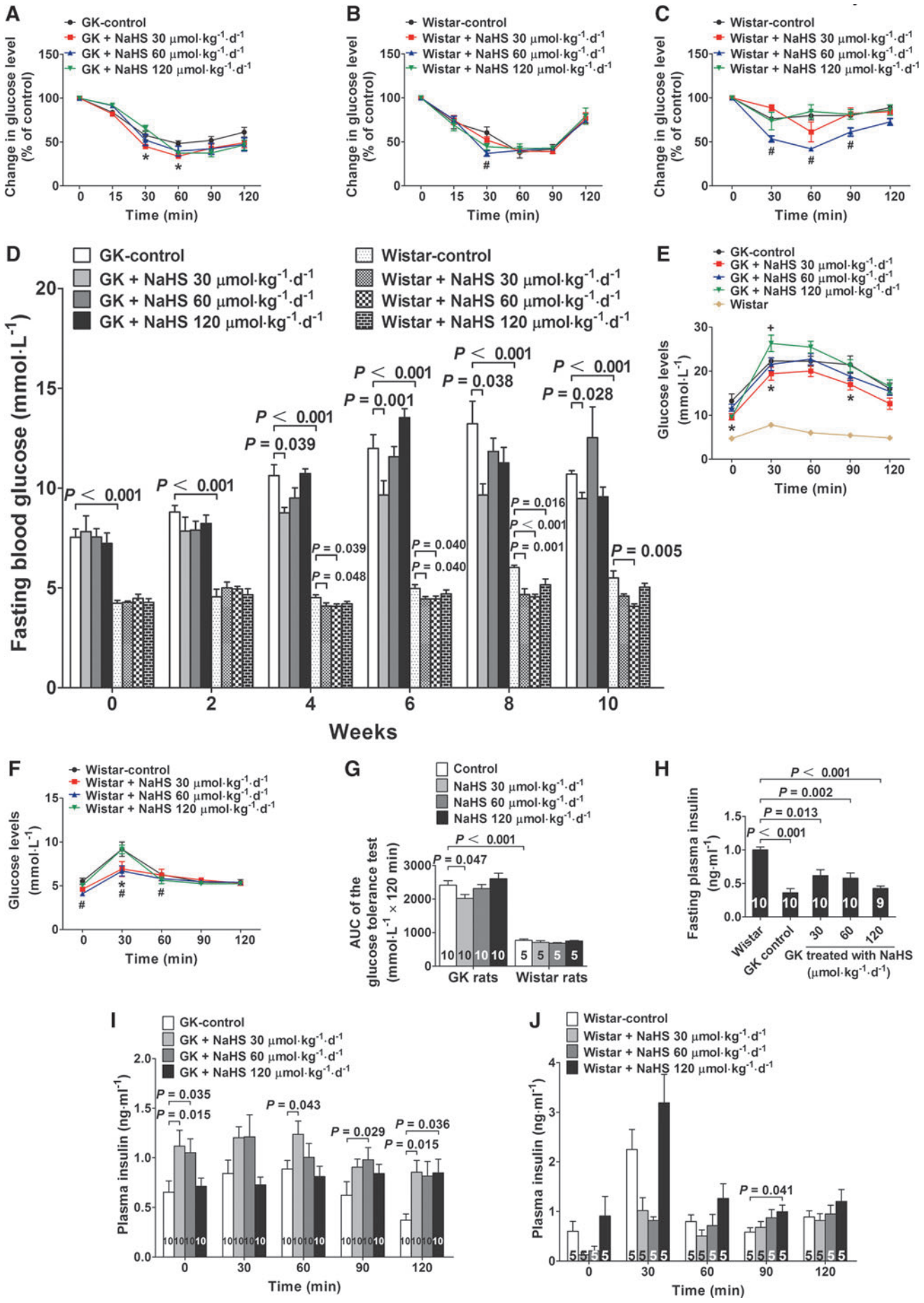
A
GK-control
GK + NaHS 30 μmol·kg-1·d-1
GK + NaHS 60 μmol·kg-1·d-1
GK + NaHS 120 μmol·kg-1·d-1
Change in glucose level (% of control)
Time (min)
B
Wistar-control
Wistar + NaHS 30 μmol·kg-1·d-1
Wistar + NaHS 60 μmol·kg-1·d-1
Wistar + NaHS 120 μmol·kg-1·d-1
Change in glucose level (% of control)
Time (min)
C
Wistar-control
Wistar + NaHS 30 μmol·kg-1·d-1
Wistar + NaHS 60 μmol·kg-1·d-1
Wistar + NaHS 120 μmol·kg-1·d-1
Change in glucose level (% of control)
Time (min)
D
GK-control
GK + NaHS 30 μmol·kg-1·d-1
GK + NaHS 60 μmol·kg-1·d-1
GK + NaHS 120 μmol·kg-1·d-1
Wistar-control
Wistar + NaHS 30 μmol·kg-1·d-1
Wistar + NaHS 60 μmol·kg-1·d-1
Wistar + NaHS 120 μmol·kg-1·d-1
Fasting blood glucose (mmol·L-1)
P < 0.001
P < 0.001
P = 0.039
P < 0.001
P = 0.001
P < 0.001
P = 0.038
P < 0.001
P = 0.028
P = 0.039
P = 0.048
P = 0.040
P = 0.040
P = 0.016
P < 0.001
P = 0.001
P = 0.005
Weeks
E
GK-control
GK + NaHS 30 μmol·kg-1·d-1
GK + NaHS 60 μmol·kg-1·d-1
GK + NaHS 120 μmol·kg-1·d-1
Wistar
Glucose levels (mmol·L-1)
Time (min)
F
Wistar-control
Wistar + NaHS 30 μmol·kg-1·d-1
Wistar + NaHS 60 μmol·kg-1·d-1
Wistar + NaHS 120 μmol·kg-1·d-1
Glucose levels (mmol·L-1)
Time (min)
G
Control
NaHS 30 μmol·kg-1·d-1
NaHS 60 μmol·kg-1·d-1
NaHS 120 μmol·kg-1·d-1
P < 0.001
P = 0.047
AUC of the glucose tolerance test (mmol·L-1 × 120 min)
GK rats
Wistar rats
H
P < 0.001
P = 0.002
P = 0.013
P < 0.001
Fasting plasma insulin (ng·ml-1)
Wistar
GK control
GK treated with NaHS (μmol·kg-1·d-1)
I
GK-control
GK + NaHS 30 μmol·kg-1·d-1
GK + NaHS 60 μmol·kg-1·d-1
GK + NaHS 120 μmol·kg-1·d-1
P = 0.035
P = 0.015
P = 0.043
P = 0.029
P = 0.036
P = 0.015
Plasma insulin (ng·ml-1)
Time (min)
J
Wistar-control
Wistar + NaHS 30 μmol·kg-1·d-1
Wistar + NaHS 60 μmol·kg-1·d-1
Wistar + NaHS 120 μmol·kg-1·d-1
P = 0.041
Plasma insulin (ng·ml-1)
Time (min)

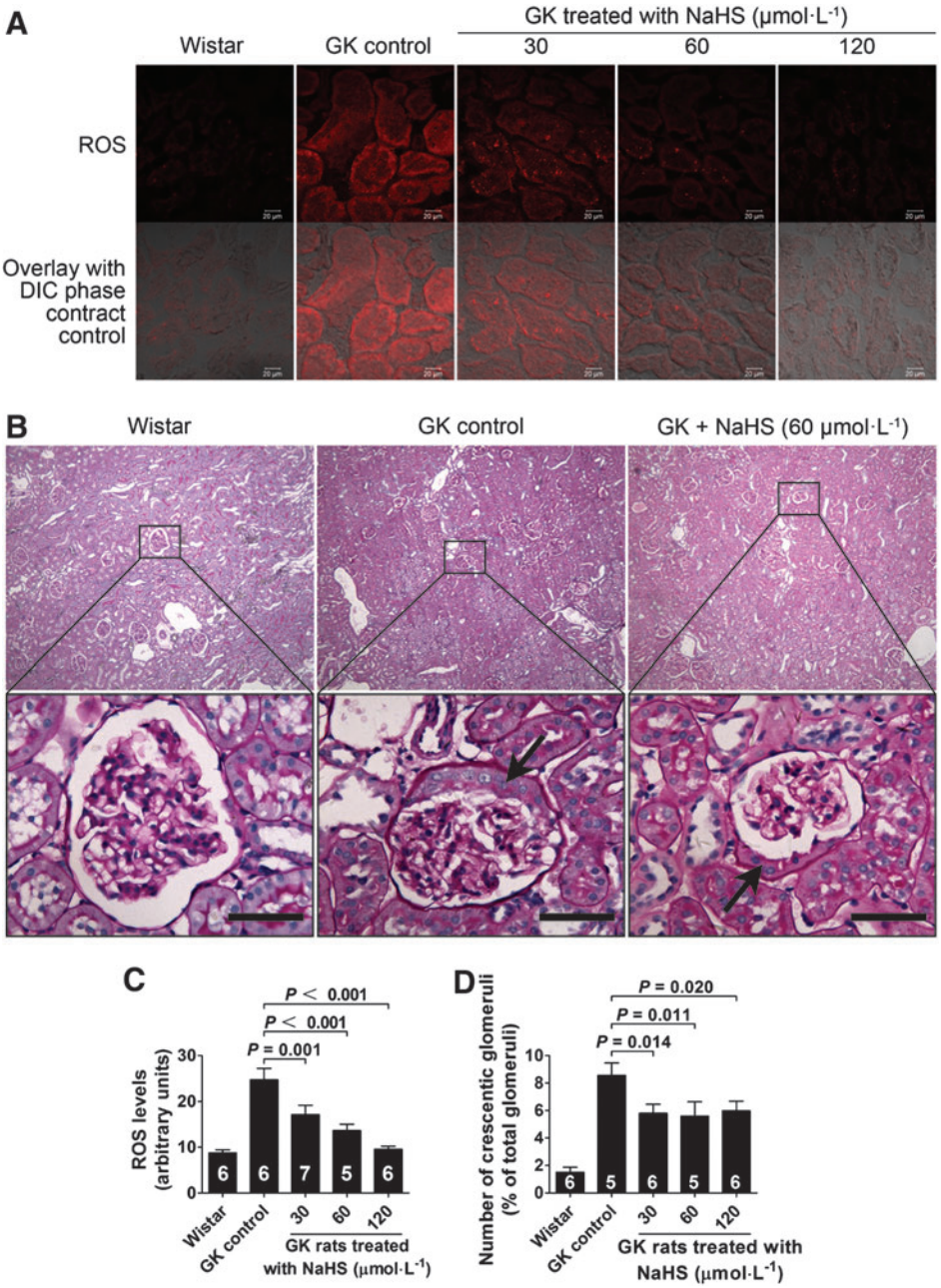

FIG. 8. Kidney morphology of the rats treated with NaHS. **(A)** Micrographs showing ROS expression in the kidney of GK rats treated with NaHS for 10 weeks. **(B)** Morphological change of the number of glomerular crescents observed in the kidney of GK rats. The number of crescentic glomeruli was decreased in the kidney of GK rats chronically treated with NaHS at doses of 30, 60, and 120 μmol·kg^{-1}·day^{-1} compared with the GK control group. Scale bar, 250 μm. **(C)** Graphs showing the statistical analysis of ROS levels in the kidney of GK rats treated with NaHS at doses of 30, 60, and 120 μmol·kg^{-1}·day^{-1}. **(D)** Graphs showing the statistical analysis of the number of crescentic glomeruli in the kidney of GK rats. Data represent means ± SE. A p value < 0.05 represents statistical significance. The arrows indicate the crescents observed in the glomeruli of GK rats. ROS, reduced oxygen species.

FIG. 7. Chronic NaHS treatment increases insulin sensitivity and glucose tolerance and decreases fasting blood glucose in both GK and Wistar rats. (A, B) Insulin sensitivity test in GK **(A)** and Wistar **(B)** rats treated with vehicle or NaHS at doses of 30, 60, and 120 μmol·kg^{-1}·day^{-1}. The rats were fasted for 12 h, followed by an insulin injection (0.75 U·kg^{-1}; i.p.). $^{*}p < 0.05$, GK 30 μmol·kg^{-1}·day^{-1} *vs.* GK control in **(A)**, $^{\#}p < 0.05$, Wistar 60 μmol·kg^{-1}·day^{-1} *vs.* Wistar control in **(B)**. **(C)** Insulin sensitivity test in Wistar rats treated with the vehicle or NaHS at doses of 30, 60, and 120 μmol·kg^{-1}·day^{-1}. The rats were fasted for 4 h, followed by an insulin injection (0.4 U·kg^{-1}; i.p.). $^{\#}p < 0.05$, Wistar 60 μmol·kg^{-1}·day^{-1} *vs.* Wistar control. **(D)** Fasting blood glucose in GK and Wistar rats during the 10-week treatment period with the vehicle or NaHS at doses of 30, 60, and 120 μmol·kg^{-1}·day^{-1}. Profile of plasma glucose levels measured during the GTT in GK **(E)** and Wistar rats **(F)** chronically treated with the vehicle or NaHS at doses of 30, 60, and 120 μmol·kg^{-1}·day^{-1}. $^{*}p < 0.05$, GK 30 μmol·kg^{-1}·day^{-1} *vs.* GK control in **(E)**, $^{+}p < 0.05$, GK 120 μmol·kg^{-1}·day^{-1} *vs.* GK control in **(E)**; $^{*}p < 0.05$, Wistar 30 μmol·kg^{-1}·day^{-1} *vs.* Wistar control in **(F)**; $^{\#}p < 0.05$, Wistar 60 μmol·kg^{-1}·day^{-1} *vs.* Wistar control in **(F)**. **(G)** The area under the curve of glucose levels of the GTT in GK and Wistar rats shown in **(E)** and **(F)**. **(H)** Fasting plasma insulin levels in GK rats treated with vehicle or NaHS at doses of 30, 60, and 120 μmol·kg^{-1}·day^{-1}. **(I, J)** Plasma insulin concentrations during the GTT in GK **(I)** and Wistar rats **(J)**. Data are means ± SE. A p value < 0.05 represents statistical significance. GK, Goto-Kakizaki; GTT, glucose tolerance test.

Table 4. Effects of Sodium Hydrosulfide Treatment for 6 Weeks on Biochemical Profiles in Goto-Kakizaki Rats

Variables	*GK control* (n = *10*)	*GK + NaHS30* (n = *10*)	*GK + NaHS60* (n = *10*)	*GK + NaHS120* (n = *10*)
Fasting blood glucose (m*M*)	11.99 ± 0.69	9.65 ± 0.72[a]	11.57 ± 0.51	13.5 ± 0.45
Total cholesterol (m*M*)	1.73 + 0.08	1.35 ± 0.13[a]	1.35 ± 0.06[a]	1.58 ± 0.05
Triglycerides (m*M*)	0.38 ± 0.02	0.47 ± 0.09	0.34 ± 0.01	0.50 ± 0.06
HDL cholesterol (m*M*)	0.67 ± 0.07	0.97 ± 0.08[a]	0.72 ± 0.22	1.03 ± 0.13[a]
LDL cholesterol (m*M*)	0.61 ± 0.12	0.33 ± 0.08[a]	0.41 ± 0.02	0.42 ± 0.08
BUN ($mg \cdot dl^{-1}$)	6.8638 ± 0.52	6.08 ± 0.4	7.8025 ± 0.49	7.9738 ± 0.40
Creatinine ($mg \cdot dl^{-1}$)	1.017 ± 0.212	0.776 ± 0.098	0.852 ± 0.044	0.737 ± 0.076
Blood pressure (mmHg)	122.75 ± 1.314	116.3 ± 4.35[a]	117.2 ± 2.39[a]	118.4 ± 2.85

[a]$p < 0.05$ *versus* control.
GK, Goto-Kakizaki; HDL, high density lipoprotein; LDL, low-density lipoprotein; BUN, blood urea nitrogen.

the diabetic animal model and the treatment protocol. GK rat is a spontaneous nonobese diabetic model with a moderate increase in blood glucose, while the Zucker diabetic rat is a transgenetic diabetic model with obesity and hyperlipidemia. In addition, we found amelioration in glucose metabolism in GK diabetic rats with chronic NaHS treatment for 10 weeks at a physiologically relevant dosage that is different from the treatment protocols of Wu *et al.* (29). The conclusion of Wu *et al.* is based on the administration of PPG, which inhibits the production of endogenous H_2S, and PPG-induced decrease in blood glucose is thereby ascribed to a decrease in endogenous H_2S. Wu *et al.* suggest that endogenous H_2S may have a role to increase blood glucose in Zucker diabetic rats. However, PPG is not a high-specific inhibitor for CSE. PPG has been shown to have some additional effects such as an inhibition on other vitamin B6-dependent enzymes (16). PPG is also a lead-containing compound, and is thus considered to be toxic after long-term administration (16). In this context, more pieces of evidence are required to draw the conclusion that endogenous H_2S may have a role to increase blood glucose in Zucker diabetic rats. Taken together, the controversy about the role of H_2S in diabetes may be ascribed to the differences in the diabetic model/animal strain, the H_2S dosage/treatment protocol, and a possible biphasic dose–response.

Interestingly, we found here that ROS expression was increased in the kidney of GK rats, and chronic NaHS treatment significantly reduced ROS expression. In addition, the number of crescentic glomeruli in the kidney of GK rats was increased as compared to the Wistar rats, and NaHS treatment reduced the number of crescentic glomeruli in the kidney of GK rats, illustrating that chronic NaHS treatment may ameliorate diabetic complications of the kidney. It is worthy of notice that we did not observe typical diabetic morphological changes such as the Kimmelstiel–Wilson nodule in the kidney of GK rats. It may be too early for these diabetic rats to develop severe glomerular fibrosis at this stage. Future studies with a much longer treatment period may help to clarify whether NaHS treatment could reduce glomerular fibrosis. Our present data can only suggest that NaHS treatment may prevent some kidney lesion at an early stage of diabetic nephropathy. Crescentic glomeruli may be induced in the high-glucose condition in the glomerular capsule. Moreover, high glucose in crude urine may also function as a stress on the nephridial tubules, and thus cause an increase in ROS in the kidney of GK rats. It is interesting that amelioration of kidney lesions was also observed in GK rats treated with NaHS at $120\,\mu mol \cdot kg^{-1} \cdot day^{-1}$, where fasting blood glucose was not decreased. The data suggest that improvement of diabetic end-organ damage is not necessarily based on normalization of blood glucose. Some neurohumoral or local pathways may be involved in the pathogenesis of the end-organ damage in diabetes irrelevant to the blood glucose levels (19, 14). NaHS may act locally in the kidney to antagonize some pathogenic pathways that are independent on the blood glucose levels. Interestingly, hepatic GSH and the ratio of GSH to GSSG were increased in GK rats chronically treated with NaHS at doses of 60 and $120\,\mu mol \cdot kg^{-1} \cdot day^{-1}$. However, NaHS treatment did not change the GSH levels nor the ratio of GSH to GSSG at a dose of $30\,\mu mol \cdot kg^{-1} \cdot day^{-1}$, which was effective in reducing fasting glucose and increasing insulin sensitivity. The data suggest that the effect of NaHS on glucose metabolism may not be dependent on a reduction of overall oxidative stress in diabetes, which may be induced by NaHS treatment at rather high doses.

The role of endogenous H_2S in regulating glucose uptake was further clarified in the present study, where siRNA-mediated knockdown of CSE caused a decrease in glucose

Table 5. Effects of Sodium Hydrosulfide Treatment for 6 Weeks on Biochemical Profiles in Wistar Rats

Variables	*Wistar control* (n = *5*)	*Wistar + NaHS30* (n = *5*)	*Wistar + NaHS60* (n = *5*)	*Wistar + NaHS 120* (n = *5*)
Fasting blood glucose (m*M*)	4.98 ± 0.19	4.46 ± 0.11[a]	4.45 ± 0.14[a]	4.7 ± 0.21
Total cholesterol (m*M*)	1.381 ± 0.088	1.078 ± 0.07[a]	1.35 ± 0.099	1.523 ± 0.07
Triglycerides (m*M*)	0.14 ± 0.021	0.11 ± 0.01[a]	0.15 ± 0.018	0.17 ± 0.012
HDL cholesterol (m*M*)	1.44 ± 0.06	1.73 ± 0.07[a]	1.45 ± 0.11	1.61 ± 0.04[a]
LDL cholesterol (m*M*)	0.26 ± 0.02	0.36 ± 0.04	0.31 ± 0.02	0.26 ± 0.01
BUN ($mg \cdot dl^{-1}$)	7.038 ± 0.15	7.65 ± 0.5	6.83 ± 0.4	5.956 ± 0.573
Creatinine ($mg \cdot dl^{-1}$)	0.31 ± 0.014	0.36 ± 0.005	0.345 ± 0.026	0.344 ± 0.008

[a]$p < 0.05$ *versus* control.
HDL, high density lipoprotein; LDL, low-density lipoprotein; BUN, blood urea nitrogen.

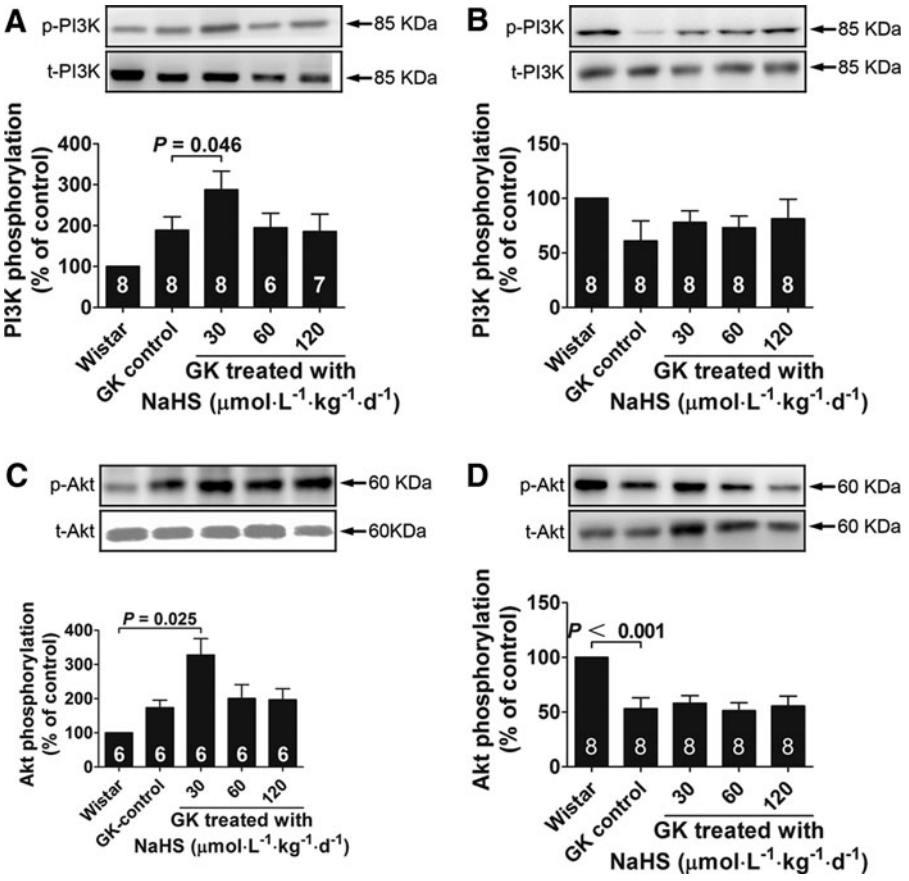

FIG. 9. Phosphorylation of PI3K and Akt in skeletal muscle and adipose tissues of the Wistar control and GK rats chronically treated with vehicle or NaHS at doses of 30, 60, and 120 μmol·kg^{-1}·day^{-1}. PI3K phosphorylation in skeletal muscle **(A)** and abdominal fat **(B)** in the Wistar control and GK rats chronically treated with NaHS. Akt phosphorylation in skeletal muscle **(C)** and abdominal fat **(D)** in the Wistar control and GK rats chronically treated with NaHS. Data represent means ± SE. A p value < 0.05 represents statistical significance.

uptake in adipocytes. This effect was more pronounced in both myotubes and adipocytes in the presence of exogenous H_2S. While the concentrations of exogenous H_2S are comparable to those found in plasma, the effects of CSE knockdown on glucose uptake in these cells may also represent a condition that is physiologically relevant. Our present data are not sufficient to clarify the mechanisms underlying the synergistic interaction between endogenous and exogenous H_2S. It is possible that the glucose uptake potency of the cells was too low to be further reduced by CSE knockdown without H_2S supplementation. When the cells were activated by exogenous H_2S, the glucose uptake potency was increased to a level that enables the cells being sensitive to a reduction of endogenous H_2S due to CSE knockdown. It is obvious that the IRs are not able to differentiate between the H_2S molecules with an endogenous or exogenous origin. However, distribution of the H_2S molecules with an endogenous and exogenous origin may be different. Exogenous H_2S may be distributed evenly in the whole cell, whereas the endogenous H_2S molecules may not be distributed evenly within the cell. The local H_2S concentration may be significantly higher in the subcellular compartments where the H_2S-generating enzymes reside than that in the subcellular compartments without the H_2S-generating enzymes. CSE may be close to the IRs, and therefore the endogenous H_2S generated from CSE may mainly affect the nearby IRs. It is possible that the interaction between endogenous and exogenous H_2S may occur in certain subcellular compartments where the IRs reside. Indeed, the current methods are not able to show the H_2S distribution in a single cell. This hypothesis remains to be examined in the future.

On the other hand, the present data are not yet sufficient to clarify the role of endogenous H_2S in the *in vivo* diabetic models. Novel approaches such as knockdown of CSE in diabetic animals may help to clarify the role of endogenous H_2S in the pathogenesis of diabetes in the future. In the present study, exogenous administration of other biological thiols such as GSH and L-cysteine was also effective in promoting glucose uptake. However, the effects of GSH and L-cysteine were weaker than NaHS in certain conditions. The mechanisms underlying these thiol effects remain to be further clarified. Although H_2S is also a reducing factor, it is not appropriate to simply conclude that the biological effects of H_2S are similar to other biological thiols. The chemical nature, metabolism, and tissue distribution of H_2S are obviously not identical to other biological thiols. In this context, the role of H_2S on glucose uptake may not be identical to that of other biological thiols. On the other hand, the mechanisms underlying the interaction between H_2S and its direct target molecule remain unknown. Our current data are not sufficient to clarify how H_2S act on its direct target molecule, for example, the IR, in the regulation of glucose metabolism, and to sort out the antioxidant from other effects of H_2S. Both NaHS and the H_2S gas solution have been applied in the present studies. H_2S gas in solution is composed of a mixture of H_2S gas and the HS^- anion that are in a dynamic equilibrium. On the other hand, NaHS also yields Na^+ and HS^- in aqueous solutions, and about two-thirds of the HS^- anions react with H^+ to yield H_2S. Therefore, either H_2S gas solution or NaHS solution contains both HS^- and H_2S.

Whether the HS^- anion or H_2S gas is the active substance to regulate glucose metabolism is unknown. On the other hand, the HS^-/H_2S ratio in the NaHS solution may not be identical to that in the H_2S solution. In this context, the slight difference in the efficiency to promote glucose uptake by NaHS and H_2S may be due to the difference in the ratio of HS^-/H_2S in these two kinds of solutions.

Innovation

This study provided the first piece of evidence for the insulin-sensitizing effect of sodium hydrosulfide/hydrogen sulfide (NaHS/H_2S) in the both *in vitro* and *in vivo* models of insulin resistance. The IRs have a pivotal role in mediating the NaHS/H_2S effects. Chronic NaHS supplementation exerts an insulin-sensitizing effect and ameliorates diabetic complications in the kidney of GK rats. These findings may be further explored to develop novel approaches for the treatment of type 2 diabetes.

Materials and Methods

Cell culture

3T3-L1 cells were cultured at 37°C in the Dulbecco's modified Eagle's medium (DMEM) containing 10% fetal bovine serum in 5% CO_2. The differentiation of 3T3-L1 cells was induced as previously described (12). The L6 myotubes were cultured and differentiated as previously described (7). Before induction of insulin resistance, adipocytes and myotubes were incubated in a low-glucose DMEM (5.5 m*M* glucose) containing 10% fetal bovine serum (FBS) for 36–48 h. Cells were incubated for a period of 24 h in either a low-glucose DMEM (5.5 m*M* glucose) containing 1% FBS and 1% (w/v) bovine serum albumin (BSA) without insulin (control cells) or a high-glucose DMEM (25 m*M* glucose) containing 1% FBS, 1% (w/v) BSA, and 100 n*M* insulin (insulin-resistant cells). Meanwhile, NaHS was added in the medium, and the control cells were treated with the vehicle, and NaHS treatment was repeated every 6 h during the entire treatment period of 24 h.

2-Deoxyglucose uptake

Uptake of 2-deoxyglucose by the 3T3-L1 adipocytes and L6 myotubes was measured as previously described after the treatment with NaHS (Sigma) at different doses (10–200 μM) for 24 h. The H_2S stock solution (10–200 μM) was freshly prepared by bubbling distilled water with pure H_2S gas (Summit Specialty Gases, Tianjin, China) to acquire a saturated H_2S solution. The cells were rinsed with a KRP buffer (128 m*M* NaCl, 4.7 m*M* KCl, 1.25 m*M* $CaCl_2$, 1.25 m*M* $MgSO_4$, 5 m*M* NaH_2PO_4, 5 m*M* Na_2HPO_4, and 10 m*M* HEPES, pH 7.4) containing 0.1% (w/v) BSA and 5 m*M* glucose every 40 min for a total of 120 min at 37°C. The cells were then treated with 100 n*M* insulin in a KRP buffer without glucose for 15 min or left untreated. 2-deoxy-D [^{3}H]-glucose (1 $\mu Ci \cdot ml^{-1}$) was added, and the cells were incubated for 15 min. The cells were rinsed three times in ice-cold phosphate-buffered saline (PBS) containing 10 m*M* glucose, and they were then lysed with 0.4 N NaOH. ^{3}H radioactivity was measured in a liquid scintillation counter (Beckman LS6500). Each sample was measured in triplicate. Nonspecific uptake was determined in the presence of cytochalasin B (10 μM) and was subtracted from each values (26). A transient treatment (15 min) with 100 n*M* insulin in the KRP buffer before the cells were treated with radioactive glucose was applied in both the cells cultured with low glucose (5.5 m*M*, without insulin) and the cells cultured with high glucose (25 m*M*) with insulin (100 n*M*). This transient insulin treatment is a necessary step for the glucose uptake assay performed for the experiments shown in Figures 1A– D, 5A–F, 6, and Supplementary Figure S10. In the experiments to examine the effect of insulin on the H_2S effects in promoting glucose uptake, the cells were cultured without insulin or with insulin at concentrations of 1, 5, 10, and 100 n*M* for 24 h (Fig. 1E–H). In these experiments, the concentration of insulin applied in the following glucose-uptake assay (including the transient insulin treatment before application of 2-deoxy-D [^{3}H]-glucose and the insulin contained after application of 2-deoxy-D [^{3}H]-glucose) was identical to that used in the cell culture period.

Western blotting

The cells were starved for 24 h and then treated for 30 min with HNMPA (300 μM) or a vehicle, followed by stimulation with 50 μM NaHS for 60 min. In another set of experiments, cells were treated either with 50 μM NaHS for various times (0–240 min) or with increasing doses of NaHS (0–200 μM) for 60 min. After NaHS treatment, cells were incubated with insulin (100 n*M*) for 15 min. For tissue samples, isolated rat muscle and abdominal fat tissue were homogenized using a polytron homogenizer. The cell and tissue samples were then washed, and the extracted protein (50 μg) was separated with gel electrophoresis, and was then transferred to a polyvinyl difluoride membrane. After blocking with TBST containing 5% milk for 1 h, the membrane was incubated with antibodies against the IR, p-IR, PI3K, p-PI3K, Akt, p-Akt (Ser473), Cbl, p-Cbl, ERK, p-ERK, Jun, p-Jun (Ser63), p38, or p-p38 overnight at 4°C. After incubation in a horseradish peroxidase-conjugated secondary antibody for 1 h, the SuperSignal West Pico Chemiluminescent Substrate was used for detection.

siRNA-mediated silencing of the IR and CSE

siRNA for the IR and CSE was provided by ABI (Applied Biosystems). L6 myotubes and 3T3-L1 adipocytes grown in 24-well plates were transiently transfected with 100 n*M* siRNA complex according to the manufacturer's instructions. Briefly, 100 n*M* siRNA specific for the IR or CSE was diluted in 100 μl Opti-MEM media (Invitrogen) and was mixed with 4–6 μl of the Lipofectamine™ 2000 transfection reagent (Invitrogen). The mixture was incubated for 30 min at room temperature to form siRNA complexes. The siRNA medium was formed by the addition of 500 μl of growth medium to the siRNA complexes. Cells were incubated with the siRNA medium for 5–6 h, followed by incubation with a fresh DMEM containing 10% FBS for 48 h. After incubation, the cells were treated with H_2S in the presence of either low level (5.5 m*M*) or high level (25 m*M*) of glucose with insulin (100 n*M*). The cells transfected with ctrl siRNA (Santa Cruz Biotechnology) served as the control. The cells were then used for the glucose-uptake assay. In another set of experiments, the lysates of cells transfected with siRNA against the IR, CSE, or control siRNA

were immunoblotted with the antibodies against the IR or CSE to examine the efficiency of siRNA-mediated silencing of the targeted genes.

Measurement of IR kinase activity

The IR kinase activity was measured by fluorescence polarization using a commercially available kit (Upstate) according to the manufacturer's instructions. Briefly, a TK substrate (787.5 μl water, 200 μl 5×Reaction Buffer [425 μl water, 500 μl 10×Kin EASE™ Buffer, 25 μl 1 M $MgCl_2$, 50 μl 0.1 *M* $MnCl_2$, and 12.5 μl 100 m*M* TK Substrate 2]), ATP (775 μl water, 200 μl 5×Reaction Buffer [425 μl water, 500 μl 10×Kin EASE™ Buffer, 25 μl 1 *M* $MgCl_2$, 50 μl 0.1 *M* $MnCl_2$, 25 μl 10 m*M* ATP]), and a recombinant human IR working solution (0.05 $U \cdot ml^{-1}$, 25$U \cdot mg^{-1}$, 10 μg of enzyme in 4.9 μl of 50 m*M* Tris/HCl, pH 7.5, 150 m*M* NaCl, 0.1 m*M* EGTA, 0.03% Brij-35, 270 m*M* sucrose, 1 m*M* benzamidine, 0.2 m*M* PMSF, and 0.1% 2-mercaptoethanol) were added to the wells. After incubation for 1 h at room temperature, the reaction was stopped using a TK stop mix (510 μl water, 280 μl 0.5 *M* EDTA, pH 7.2, and 200 μl 5×Detection Buffer [250 m*M* HEPES, pH 7.2, 0.5% Tween®-20, 5 m*M* DTT], and 10 μl 100×TK Tracer). After 4-h incubation at room temperature with the TK antibody [750 μl water and 200 μl 5×Detection Buffer (425 μl water, 500 μl 10×Kin EASE™ Buffer, 25 μl 1 *M* $MgCl_2$, 50 μl 0.1 *M* $MnCl_2$, and 50 μl 20×TK antibodies)], the fluorescence polarization value was detected by a plate reader (Molecular Devices Corporation).

Measurement of PTP activity

The PTP1B activity was measured with a colorimetric method using a commercially available kit (Merck) according to the manufacturer's instructions. Briefly, the PTP1B enzyme was mixed with an assay buffer and various concentrations of NaHS. Suramin (10 μM) was added as a positive control of PTP1B inhibition. After incubation for 30 min at room temperature, the reaction was terminated with a phosphate detection reagent. After color developing, the absorbance at 620 nm was measured with a spectrophotometer (Tecan).

Animal models

Eight-week-old male GK rats and male Wistar rats weighing 250 g (obtained from the Department of Experimental Animals at the Chinese Academy of Sciences) were randomly assigned to eight groups as follows: GK control (GK rats treated with saline; 1 $ml \cdot kg^{-1} \cdot day^{-1}$; i.p.), GK-NaHS30 (GK rats treated with NaHS; 30 $\mu mol \cdot kg^{-1} \cdot day^{-1}$; i.p.), GK-NaHS60 (GK rats treated with NaHS; 60 $\mu mol \cdot kg^{-1} \cdot day^{-1}$; i.p.), GK-NaHS120 (GK rats treated with NaHS; 120 $\mu mol \cdot kg^{-1} \cdot day^{-1}$; i.p.), and Wistar control (Wistar rats treated with saline; 1 $ml \cdot kg^{-1} \cdot day^{-1}$; i.p.), Wistar-NaHS30 (Wistar rats treated with NaHS; 30 $\mu mol \cdot kg^{-1} \cdot day^{-1}$; i.p.), Wistar-NaHS60 (Wistar rats treated with NaHS; 60 $\mu mol \cdot kg^{-1} \cdot day^{-1}$; i.p.), and Wistar-NaHS120 (Wistar rats treated with NaHS; 120 $\mu mol \cdot kg^{-1} \cdot day^{-1}$; i.p.). H_2S was administered in the form of NaHS (Sigma), which has been well established as a reliable donor of H_2S (23, 28). The NaHS solutions (30, 60, and 120 $\mu mol \cdot ml^{-1}$) were freshly prepared before use. The rats were treated once a day for 10 weeks.

The *in vivo* experiments were performed according to the Guide for the Care and Use of Laboratory Animals published by the National Institutes of Health (NIH) of the United States and were approved by the Ethics Committee of Experimental Research, Fudan University Shanghai Medical College.

Fasted plasma parameters

After the rats were fasted overnight, the blood samples (200 μl) were taken in heparin-coated tubes via tail bleeding from the different groups, and plasma was collected by centrifugation. The glucose levels were monitored using the blood glucose strips (Onetouch; Johnson). TGs and total cholesterol were determined using commercially available kits (Jian-Cheng) according to the manufacturers' instructions. Plasma insulin was measured by a radioimmunoassay using rat insulin standards (Sensitive Rat Insulin Assay; Linco Research).

GTT and insulin tolerance test

After a 12-h fast, the GTT was conducted by intraperitoneally injecting the rats with 1.5 g of dextrose per kilogram of body weight using a 25% dextrose solution. Blood samples were collected from the tails at different times (0, 30, 60, 90, and 120 min) for glucose and insulin measurement after dextrose injection. The glucose levels were monitored using the blood glucose strips (Onetouch; Johnson). For the insulin tolerance test (ITT), the rats were fasted for 12 h followed by an insulin injection (0.75 $U \cdot kg^{-1}$; i.p.). The blood glucose levels were assessed before and 15, 30, 60, 90, and 120 min into the ITTs (9). The GTT and the insulin sensitivity test were performed 2–4 h after the NaHS injection.

Morphological examination of the kidney

Paraffin-embedded kidney tissues were cut into 7-μm frontal sections and stained with periodic acid–Schiff. The slides were examined by an observer blinded to the treatment groups, and the glomeruli in each field of one section was carefully examined and counted. About 300 glomeruli were found in each section, and the number of glomerular crescents was also counted. The ratio of glomerular crescents to glomeruli was calculated in each section.

ROS expression was measured using dihydroethidium (DHE) staining (Sigma-Aldrich) to evaluate the *in situ* levels of superoxide (O^{2-}) in the kidney. Briefly, the kidney frozen-tissue sections (10 μm) were incubated with 10 μM DHE at 37°C for 30 min in a light-tight humidified chamber. Then, the slides were washed with PBS for three times, and covered with a mounting medium. The average of 6 sections stained with DHE was taken as the value for each animal. The sections were observed using a Zeiss confocal microscope (Zeiss LSM710) with the wavelength of 488/585 nm.

Measurement of GSH and GSSG levels

The concentrations of total GSH (T-GSH), reduced GSH, and oxidized disulfide (GSSG) were measured by an enzymatic method according to the commercial assay kit procedure (Beyotime Institute of Biotechnology). Briefly, 10 mg rat liver or muscle tissue was homogenized in a protein removal reagent and then centrifuged at 10,000 *g* for 10 min at 4°C. The supernatant was used for the assay of GSH and

GSSG. The T-GSH level was measured by the method of the dithio-bis-nitrobenzoic acid (DTNB)-GSSG recycling assay (1). GSSG was measured by detecting 5-thio-2-nitrobenzoic acid (TNB), which was produced from the reaction of reduced GSH with DTNB. The rate of TNB formation was measured by the absorbance at 412 nm (Tecan M200). The amount of reduced GSH was obtained by subtracting the amount of GSSG from that of the T-GSH.

Statistical analysis

Results were expressed as means ± standard error. Differences between the groups were analyzed by one-way ANOVA followed by *post hoc* Tukey's test where applicable. The AUC of glucose levels was calculated according to the trapezoidal rule. Significance was established at the $p < 0.05$ level.

Acknowledgments

This work was supported by grants from the Ministry of Science and Technology (2010CB912601 and 2012ZX0950 1001-001-002) of China, the Ministry of Education (20110 071130009), and the National Natural Science Foundation of China (81230003, 30825016, and 30971064). We thank Prof. Jin-Sheng Zhang for his critical comments on the morphological examination.

Author Disclosure Statement

No competing financial interests exist.

References

1. Baker MA, Cerniglia GJ, and Zaman A. Microtiter plate assay for the measurement of glutathione and glutathione disulfide in large numbers of biological samples. *Anal Biochem* 190: 360–365, 1990.
2. Brancaleone V, Roviezzo F, Vellecco V, De Gruttola L, Bucci M, and Cirino G. Biosynthesis of H_2S is impaired in non-obese diabetic (NOD) mice. *Br J Pharmacol* 155: 673–680, 2008.
3. Cai WJ, Wang MJ, Moore PK, Jin HM, Yao T, and Zhu YC. The novel proangiogenic effect of hydrogen sulfide is dependent on Akt phosphorylation. *Cardiovasc Res* 76: 29–40, 2007.
4. Feng X, Chen Y, Zhao J, Tang C, Jiang Z, and Geng B. Hydrogen sulfide from adipose tissue is a novel insulin resistance regulator. *Biochem Biophys Res Commun* 380: 153–159, 2009.
5. Giacco F, Perruolo G, D'Agostino E, Fratellanza G, Perna E, Misso S, Saldalamacchia G, Oriente F, Fiory F, Miele C, Formisano S, Beguinot F, and Formisano P. Thrombin-activated platelets induce proliferation of human skin fibroblasts by stimulating autocrine production of insulin-like growth factor-1. *FASEB J* 20: 2402–2404, 2006.
6. Goldstein BJ, Bittner-Kowalczyk A, White MF, and Harbeck M. Tyrosine dephosphorylation and deactivation of insulin receptor substrate-1 by protein-tyrosine phosphatase 1B. Possible facilitation by the formation of a ternary complex with the GRB2 adaptor protein. *J Biol Chem* 275: 4283–4289, 2000.
7. Huang C, Somwar R, Patel N, Niu W, Torok D, and Klip A. Sustained exposure of L6 myotubes to high glucose and insulin decreases insulin-stimulated GLUT4 translocation but upregulates GLUT4 activity. *Diabetes* 51: 2090–2098, 2002.
8. Ji Y, Pang QF, Xu G, Wang L, Wang JK, and Zeng YM. Exogenous hydrogen sulfide postconditioning protects isolated rat hearts against ischemia-reperfusion injury. *Eur J Pharmacol* 587: 1–7, 2008.
9. Joseph JW, Koshkin V, Zhang CY, Wang J, Lowell BB, Chan CB, and Wheeler MB. Uncoupling protein 2 knockout mice have enhanced insulin secretory capacity after a high-fat diet. *Diabetes* 51: 3211–3219, 2002.
10. Kamoun P. Endogenous production of hydrogen sulfide in mammals. *Amino Acids* 26: 243–254, 2004.
11. Khan AH and Pessin JE. Insulin regulation of glucose uptake: a complex interplay of intracellular signalling pathways. *Diabetologia* 45: 1475–1483, 2002.
12. Kim JB and Spiegelman BM. ADD1/SREBP1 promotes adipocyte differentiation and gene expression linked to fatty acid metabolism. *Genes Dev* 10: 1096–1107, 1996.
13. Kumar N and Dey CS. Metformin enhances insulin signalling in insulin-dependent and-independent pathways in insulin resistant muscle cells. *Br J Pharmacol* 137: 329–336, 2002.
14. Lautt WW. The HISS story overview: a novel hepatic neurohumoral regulation of peripheral insulin sensitivity in health and diabetes. *Can J Physiol Pharmacol.* 77: 553–562, 1999.
15. Lefer DJ. Potential importance of alterations in hydrogen sulphide (H_2S) bioavailability in diabetes. *Br J Pharmacol* 155: 617–619, 2008.
16. Lowicka E, Bełtowski J. Hydrogen sulfide (H_2S)—the third gas of interest for pharmacologists. *Pharmacol Rep* 59: 4–24, 2007.
17. Olefsky JM. Treatment of insulin resistance with peroxisome proliferator-activated receptor gamma agonists. *J Clin Invest* 106: 467–472, 2000.
18. Pan TT, Chen YQ, and Bian JS. All in the timing: a comparison between the cardioprotection induced by H_2S preconditioning and post-infarction treatment. *Eur J Pharmacol* 616: 160–165, 2009.
19. Pliquett RU, Fasshauer M, Blüher M, Paschke R. Neurohumoral stimulation in type-2-diabetes as an emerging disease concept. *Cardiovasc Diabetol* 3: 1–8, 2004.
20. Saad MF, Knowler WC, Pettitt DJ, Nelson RG, Mott DM, and Bennett PH. Sequential changes in serum insulin concentration during development of non-insulin-dependent diabetes. *Lancet* 1: 1356–1359, 1989.
21. Saltiel AR and Kahn CR. Insulin signalling and the regulation of glucose and lipid metabolism. *Nature* 414: 799–806, 2001.
22. Saltiel AR and Pessin JE. Insulin signaling pathways in time and space. *Trends Cell Biol* 12: 65–71, 2002.
23. Shi YX, Chen Y, Zhu YZ, Huang GY, Moore PK, Huang SH, Yao T, and Zhu YC. Chronic sodium hydrosulfide treatment decreases medial thickening of intramyocardial coronary arterioles, interstitial fibrosis, and ROS production in spontaneously hypertensive rats. *Am J Physiol Heart Circ Physiol* 293: 2093–2100, 2007.
24. Smit L and Borst J. The Cbl family of signal transduction molecules. *Crit Rev Oncog* 8: 359–379, 1997.
25. Sun YG, Cao YX, Wang WW, Ma SF, Yao T, and Zhu YC. Hydrogen sulphide is an inhibitor of L-type calcium channels and mechanical contraction in rat cardiomyocytes. *Cardiovasc Res* 79: 632–641, 2008.
26. Thomson MJ, Williams MG, and Frost SC. Development of insulin resistance in 3T3-L1 adipocytes. *J Biol Chem* 272: 7759–7764, 1997.
27. Wang R. Hydrogen sulfide: the third gasotransmitter in biology and medicine. *Antioxid Redox Signal* 12: 1061–1064, 2010.

28. Wang MJ, Cai WJ, Li N, Ding YJ, Chen Y, and Zhu YC. The hydrogen sulfide donor NaHS promotes angiogenesis in a rat model of hind limb ischemia. *Antioxid Redox Signal* 12: 1065–1077, 2010.
29. Wu L, Yang W, Jia X, Yang G, Duridanova D, Cao K, and Wang R. Pancreatic islet overproduction of H_2S and suppressed insulin release in Zucker diabetic rats. *Lab Invest* 89: 59–67, 2009.
30. Yao LL, Huang XW, Wang YG, Cao YX, Zhang CC, and Zhu YC. Hydrogen sulfide protects cardiomyocytes from hypoxia/reoxygenation-induced apoptosis by preventing GSK-3beta-dependent opening of mPTP. *Am J Physiol Heart Circ Physiol* 298:H1310–1319, 2010.
31. Yusuf M, Kwong Huat BT, Hsu A, Whiteman M, Bhatia M, and Moore PK. Streptozotocin-induced diabetes in the rat is associated with enhanced tissue hydrogen sulfide biosynthesis. *Biochem Biophys Res Commun* 333: 1146–1152, 2005.
32. Zhong G, Chen F, Cheng Y, Tang C, and Du J. The role of hydrogen sulfide generation in the pathogenesis of hypertension in rats induced by inhibition of nitric oxide synthase. *J Hypertens* 21: 1879–1885, 2003.

Address correspondence to:
Prof. Yi-Chun Zhu
Department of Physiology and Pathophysiology
Fudan University Shanghai Medical College
138 Yi Xue Yuan Road
Shanghai 200032
China
E-mail: yczhu@shmu.edu.cn

Date of first submission to ARS Central, October 23, 2012; date of final revised submission, December 23, 2012; date of acceptance, January 5, 2013.

Abbreviations Used

AUC = area under curve
BSA = bovine serum albumin
BUN = blood urea nitrogen
CBS = cystathionine β-synthase
CSE = cystathionine γ-lyase
DHE = dihydroethidium
DMEM = Dulbecco's modified Eagle's medium
DTNB = dithio-bis-nitrobenzoic acid
FBS = fetal bovine serum
GK = Goto-Kakizaki
GSH = glutathione
GTT = glucose tolerance test
H_2S = hydrogen sulfide
HDL = high density lipoprotein
IR = insulin receptor
ITT = insulin tolerance test
LDL = low density lipoprotein
NaHS = sodium hydrosulfide
PBS = phosphate-buffered saline
PTP1B = protein tyrosine phosphatase 1B
ROS = reduced oxygen species
SE = standard error
TG = triglycerides
TNB = 5-thio-2-nitrobenzoic acid